

# Instability of three-band Tomonaga-Luttinger liquid: renormalization group analysis and possible application to $\text{K}_2\text{Cr}_3\text{As}_3$

Jian-Jian Miao,<sup>1,2</sup> Fu-Chun Zhang,<sup>1,2</sup> and Yi Zhou<sup>1,2</sup>

<sup>1</sup>*Department of Physics, Zhejiang University, Hangzhou 310027, China*

<sup>2</sup>*Collaborative Innovation Center of Advanced Microstructures, Nanjing 210093, China*

(Dated: December 3, 2024)

Motivated by recently discovered quasi-one-dimensional superconductor  $\text{K}_2\text{Cr}_3\text{As}_3$  with  $D_{3h}$  lattice symmetry, we study one-dimensional three-orbital Hubbard model with generic electron repulsive interaction described by intra-orbital repulsion  $U$ , inter-orbital repulsion, and Hund's coupling  $J$ . As extracted from density functional theory calculation, two of the three atomic orbitals are degenerate ( $E'$  states) and the third one is non-degenerate ( $A'_1$ ), and the system is presumed to be at an incommensurate filling. With the help of bosonization, we have usual three-band Tomonaga-Luttinger liquid for the normal state. Possible charge density wave (CDW), spin density wave (SDW) and superconducting (SC) instabilities are analyzed by renormalization group. The ground state depends on the ratio  $J/U$  and is sensitive to the degeneracy of  $E'$  bands. At  $0 < J < U/3$ , spin-singlet SC state is favored, while spin-triplet superconductivity will be favored in the region  $U/3 < J < U/2$ . The SDW state has the lowest energy only in the unphysical parameter region  $J > U/2$ . When the two-fold degeneracy of  $E'$  bands is lifted, SDW instability has the tendency to dominate over the spin-singlet SC state at  $0 < J < U/3$ , while the order parameter of the spin-triplet SC state will be modulated by a phase factor  $2\Delta k_F x$  at  $U/3 < J < U/2$ . Possible experimental consequences and applications to  $\text{K}_2\text{Cr}_3\text{As}_3$  are discussed.

PACS numbers: 74.20.-z; 74.70.-b; 71.10.Fd; 71.10.Pm

## I. INTRODUCTION

There has been considerable interest on the recent discovery of a new family of quasi-one-dimensional (quasi-1D) unconventional superconductors  $\text{A}_2\text{Cr}_3\text{As}_3$  ( $\text{A} = \text{K}, \text{Rb}, \text{Cs}$ ) in ambient pressure with  $T_c$  up to  $6.1 \text{ K}$ <sup>1-3</sup>, because of their exotic properties revealed in various experiments below. (1) In the normal state, the resistivity in polycrystalline samples follows linear temperature dependence,  $\rho(T) = \rho_0 + AT$ , in a wide temperature region, different from the usual Fermi liquid behavior  $\rho_0 + AT$ <sup>21-3</sup>. On the other hand, the transport measurement in single crystalline samples indicates that the normal state is a smectic metal, namely, it behaves as a metal along the  $c$ -axis and a semiconductor on the  $ab$ -plane<sup>4</sup>. (2) Nuclear magnetic resonance (NMR) and nuclear quadrupole resonance (NQR) measurements on  $\text{K}_2\text{Cr}_3\text{As}_3$  show a non-integer power-law temperature dependent  $1/T_1 \sim T^{0.75}$  above  $T_c$ , which is neither  $1/T_1 \sim T$  for a Fermi liquid nor Curie-Weiss behavior  $1/T_1 T \sim C/(T + \theta)$  for a ferromagnet or antiferromagnet<sup>5</sup>. Meanwhile, NMR and NQR experiments on  $\text{Rb}_2\text{Cr}_3\text{As}_3$  show a critical spin fluctuation above  $T_c$ ,  $1/T_1 T \sim a + b/(T + \theta)$ , where  $\theta \sim 0 \text{ K}$ <sup>6</sup>. The Hebel-Slichter coherence peak of  $1/T_1$  is absent in both compounds. (3)  $\text{K}_2\text{Cr}_3\text{As}_3$  possesses a large upper critical field  $H_{c2}$ , which exceeds the BCS weak-coupling Pauli limit field by 3-4 times<sup>1,7,8</sup>. The angle resolved  $H_{c2}$  measurement demonstrates strong anisotropy and reveals dominant spin-triplet SC pairing<sup>9</sup>, which is consistent with the observation of a very weak spontaneous internal magnetic field near  $T_c$  in the muon spin relaxation/rotation ( $\mu\text{SR}$ ) experiment<sup>10</sup>. (4) London penetration depth measurement for  $\text{K}_2\text{Cr}_3\text{As}_3$  shows linear

temperature dependence,  $\Delta\lambda(T) \sim T$ , at temperatures  $T \ll T_c$ , indicating the existence of line nodes in the SC gap<sup>11</sup>. (5) Doping nonmagnetic impurities in  $\text{K}_2\text{Cr}_3\text{As}_3$  will reduce  $T_c$  significantly, which indicates non- $s$ -wave superconductivity<sup>12</sup>.

There have also been a series of theoretical studies. (1) The electronic structure of  $\text{K}_2\text{Cr}_3\text{As}_3$  has been investigated by Jiang *et al.*<sup>13</sup> using density functional theory (DFT), which is confirmed by later calculation<sup>14</sup>. The band calculations show that Cr- $3d$  orbitals dominate the electronic states near the Fermi level, and there exist three energy bands at the Fermi level: two quasi-1D  $\alpha$ - and  $\beta$ -bands with flat Fermi surfaces, and a 3D  $\gamma$ -band. (2) Zhou *et al.* proposed a minimum effective model based on three molecular orbitals on a hexagonal lattice with  $D_{3h}$  symmetry<sup>15</sup>. They found that for small Hubbard  $U$  and moderate Hund's coupling  $J$ , the pairing arises from the 3D  $\gamma$  band and has a spatial symmetry  $f_{y(3x^2-y^2)}$ , which gives line nodes in the gap function, while for large  $U$ , a fully gapped  $p$ -wave state,  $p_z \hat{z}$  dominates at the quasi-1D  $\alpha$ -band. The spin-triplet SC pairing is driven by the Hund's coupling. Similar three-band and six-band models are also proposed by Wu *et al.*<sup>16-18</sup>. The dominant SC instability channels are found as  $p_z$  and  $f_{y(3x^2-y^2)}$  for weak and strong Hund's coupling respectively. (3) Zhong *et al.* carried out DFT calculation on a single  $[\text{CrAs}]_\infty$  tube to construct an effective three-band Hubbard model<sup>19</sup>. Possible Luttinger liquid instabilities have been proposed based on such a three-band Hubbard chain.

Beside its possible exotic superconductivity,  $\text{K}_2\text{Cr}_3\text{As}_3$  provides an unique platform for us to study 1D correlated electrons apart from carbon nanotubes and

cuprate ladders. The key building block of  $\text{K}_2\text{Cr}_3\text{As}_3$  is the 1D  $[(\text{Cr}_3\text{As}_3)^{2-}]_\infty$  double-walled subnanotubes, which are separated by columns of  $\text{K}^+$  ions, in contrast to the layered iron-pnictide and copper-oxide high Tc superconductors<sup>1</sup>. These  $[(\text{Cr}_3\text{As}_3)^{2-}]_\infty$  tubes together with  $\text{K}^+$  ions form a noncentrosymmetric hexagonal lattice with  $D_{3h}$  point group<sup>1</sup>. The quasi-one-dimensionality can be also seen from its electronic structure, say, the existence of two quasi-1D electron bands<sup>13,14</sup>. Experimentally, both the smectically metallic transport<sup>4</sup> and the non-integer power-law temperature dependence in NMR  $1/T_1 \sim T^{0.755}$  imply a Tomonaga-Luttinger liquid (TLL) normal state. The question is how this three-band TLL normal state gives rise to the unconventional SC states below  $T_c$ . This motivates us to study possible instabilities of three-band TLLs in this paper.

It is noted that two-leg Hubbard ladders and two-orbital Hubbard chains have been investigated in previous studies<sup>20,21</sup>, and that the SC instability caused by electron-phonon coupling in three-band metallic nanotubes has also been theoretically investigated<sup>22</sup>. In this paper, we shall focus on electron interactions in a 1D three-band Hubbard model.

This paper is organized as follows. We present the electronic model Hamiltonian in Section II. In Section III, the low-energy scattering processes near the Fermi points are classified by using generalized  $g$ -ology. In Section IV, we take the continuum limit and use bosonization technique to transform the fermionic Hamiltonian into bosonic Hamiltonian. The non-interacting part describes a three-band Tomonaga-Luttinger liquid. The remaining terms make up the bosonic interaction. In Section V, order parameters are defined to characterize ordered states. In Section VI, we utilize renormalization group (RG) to analyze these bosonic interaction. The RG equations are derived by operator product expansion (OPE) method. The relevant terms lead to different instabilities in different parameters regions. Section VII is devoted to discussions and conclusions.

## II. MODEL HAMILTONIAN

We consider a single fermionic chain with a unit cell (per  $\text{Cr}_6\text{As}_6$  cluster) containing three molecular orbitals. One of the three orbitals belongs to one-dimensional irreducible representation  $A'$  of  $D_{3h}$  group, and the other two are in the two-dimensional irreducible representation  $E'$ <sup>15</sup>. Without loss of generality, the fermionic Hamiltonian contains two parts,

$$H^F = H_0^F + H_{int}^F, \quad (1a)$$

where the non-interacting part  $H_0^F$  is a three-band tight-binding Hamiltonian describing the electron hopping, while the interacting part  $H_{int}^F$  originates from the electron-electron interaction.

The  $D_{3h}$  lattice symmetry do not allow the mixture between  $A'_1$  state and  $E'$  states along the  $c$ -direction. The absence of such hybridization is also seen from the DFT calculation, where the  $\beta$  and  $\gamma$  bands are degenerate along the  $\Gamma - A$  line. Neglecting the inter-chain coupling, we have the following  $H_0^F$  in such a one-dimensional system,

$$H_0^F = \sum_{km\sigma} \xi_{km} c_{km\sigma}^\dagger c_{km\sigma}, \quad (1b)$$

where  $m = 0, \pm 1$  is the orbital (and also band) index and  $\sigma = \uparrow, \downarrow$  is the spin index. Explicitly,  $m = 0$  refers to the  $A'_1$  state and  $m = \pm 1$  refers to  $E'$  states.  $c_{km\sigma}$  ( $c_{km\sigma}^\dagger$ ) is electron annihilation (creation) operator for orbital  $m$  and spin  $\sigma$ . The energy dispersion  $\xi_{km}$  can be linearized near the Fermi energy, as is sketched in Fig. 1.

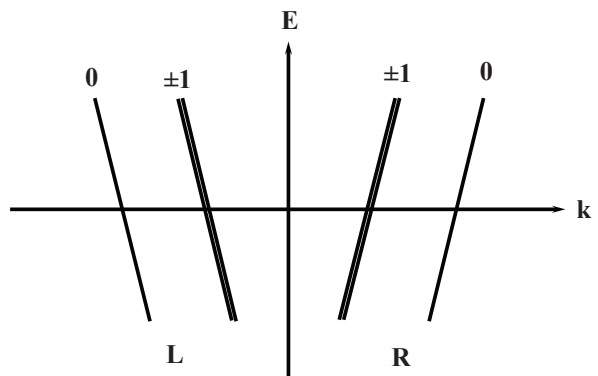


FIG. 1. Energy dispersion near the Fermi energy.

The interacting part  $H_{int}^F$  describes electron interactions. In the Hubbard approximation, we only retain on-site Coulomb repulsion. The interaction Hamiltonian contains four terms

$$\begin{aligned} H_{int}^F = & \frac{1}{2} \sum_{im} \sum_{\sigma \neq \sigma'} U n_{im\sigma} n_{im\sigma'} + \frac{1}{2} \sum_{i\sigma'} \sum_{m \neq m'} U' n_{im\sigma} n_{im'\sigma'} \\ & - \sum_i \sum_{m \neq m'} J \left( \vec{S}_{im} \cdot \vec{S}_{im'} + \frac{1}{4} n_{im} n_{im'} \right) \\ & + \frac{1}{2} \sum_{i\sigma} \sum_{m \neq m'} J' c_{im\sigma}^\dagger c_{im\bar{\sigma}}^\dagger c_{im'\bar{\sigma}} c_{im'\sigma}, \end{aligned} \quad (1c)$$

where  $n_{im\sigma} = c_{im\sigma}^\dagger c_{im\sigma}$ ,  $n_{im} = \sum_{\sigma} n_{im\sigma}$ ,  $\vec{S}_{im} = \frac{1}{2} \sum_{\alpha\beta} c_{im\alpha}^\dagger \vec{\tau}_{\alpha\beta} c_{im\beta}$ ,  $\vec{\tau}$  is a vector with three components of Pauli matrices, and  $\bar{\sigma} = -\sigma$  is the opposite spin to  $\sigma$ .  $U$  is the intra-orbital repulsion,  $U'$  is the inter-orbital repulsion,  $J$  is the Hund's coupling, and  $J'$  is the pair-hopping. Note that we have chosen Wannier functions to be real. The two degenerate orbitals  $m = \pm 1$  transfer as  $x$  and  $y$  under  $D_{3h}$  symmetry operations respectively. We also assume that

$$J' = J > 0, \quad (2)$$

such that the following relation

$$U = U' + 2J \quad (3)$$

arises subject to the rotational symmetry of the Coulomb interaction.

### III. CONTINUUM LIMIT AND THE $g$ -OLOGY

Now we introduce electron fields  $c_{m\sigma}(x)$  to study the low energy physics in the continuum limit, hereafter  $x$  denotes the coordinate along the chain ( $c$ -direction). In a one-dimensional system, Fermi points fall into two categories characterized by chirality  $p = R, L$ , which represent right and left-moving electrons respectively. Thus the electron field  $c_{m\sigma}(x)$  can be decomposed into two parts

$$c_{m\sigma}(x) = \psi_{Rm\sigma}(x) + \psi_{Lm\sigma}(x) \quad (4)$$

in low energies.

In order to classify various scattering processes in such a three-band system, we shall generalize the conventional  $g$ -ology<sup>21,23</sup> for single-band spinless fermions, which now includes chirality, band and spin indices. For single-band spinless fermions, there are four possible scattering processes between the two chiralities because of lattice momentum conservation. All these scattering processes are illustrated in Fig. 2, back scattering  $g^{(1)}\psi_p^\dagger\psi_{\bar{p}}^\dagger\psi_p\psi_{\bar{p}}$ , double-chirality forward scattering  $g^{(2)}\psi_p^\dagger\psi_{\bar{p}}^\dagger\psi_{\bar{p}}\psi_p$ , umklapp scattering  $g^{(3)}\psi_{\bar{p}}^\dagger\psi_p^\dagger\psi_{\bar{p}}\psi_{\bar{p}}$  and single-chirality forward scattering  $g^{(4)}\psi_p^\dagger\psi_p^\dagger\psi_p\psi_p$ , where  $\bar{p}$  is the opposite chirality to  $p$ .

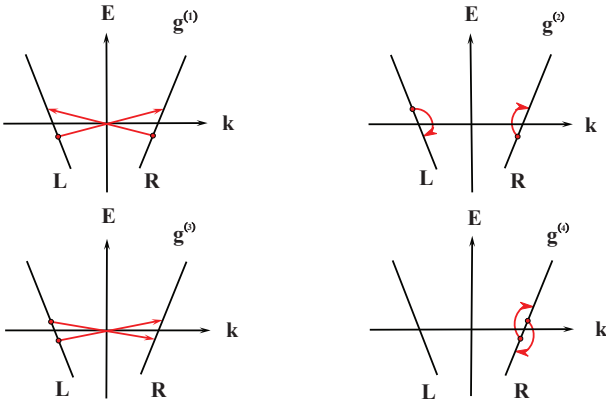


FIG. 2. Four possible scattering processes for single-band spinless fermions:  $g^{(1)}\psi_p^\dagger\psi_{\bar{p}}^\dagger\psi_p\psi_{\bar{p}}$ ,  $g^{(2)}\psi_p^\dagger\psi_{\bar{p}}^\dagger\psi_{\bar{p}}\psi_p$ ,  $g^{(3)}\psi_{\bar{p}}^\dagger\psi_p^\dagger\psi_{\bar{p}}\psi_{\bar{p}}$  and  $g^{(4)}\psi_p^\dagger\psi_p^\dagger\psi_p\psi_p$ , where  $\bar{p}$  is the opposite chirality to  $p$ .

For the three-band spinful fermions, we introduce one more notation  $f$  and two more subscripts to describe the scattering processes beside the existing superscript, which is summarized in Table I. One of the subscripts

is for spin degrees of freedom, namely, “ $\parallel$ ” denotes spin parallel scatterings and “ $\perp$ ” denotes spin anti-parallel scatterings. The other subscript is associated with the notations  $g$  and  $f$ . Now the notation  $g$  is used only for the scattering processes within the same  $D_{3h}$  irreducible representation, which includes the scatterings between two  $E'$  bands with  $m = \pm 1$  and the scatterings within the  $A'_1$  band with  $m = 0$ . It is similar to  $g^{1,2,3,4}$  for two chiralities that we use  $g_1\psi_m^\dagger\psi_{\bar{m}}^\dagger\psi_m\psi_{\bar{m}}$ ,  $g_2\psi_m^\dagger\psi_{\bar{m}}^\dagger\psi_{\bar{m}}\psi_m$ ,  $g_3\psi_m^\dagger\psi_m^\dagger\psi_{\bar{m}}\psi_{\bar{m}}$ , and  $g_4\psi_m^\dagger\psi_m^\dagger\psi_m\psi_m$  for the scatterings between two  $E'$  bands, where  $\bar{m}$  is the opposite orbital to  $m$ . We also use  $g\psi_0^\dagger\psi_0^\dagger\psi_0\psi_0$  for the scattering within the  $A'_1$  band by neglecting the subscript. On the other hand, the new notation  $f$  describes the scatterings between  $E'$  and  $A'_1$  bands, including  $f_1(\psi_m^\dagger\psi_0^\dagger\psi_m\psi_0 + h.c.)$ ,  $f_2(\psi_m^\dagger\psi_0^\dagger\psi_0\psi_m + h.c.)$ , and  $f_3(\psi_m^\dagger\psi_m^\dagger\psi_0\psi_0 + h.c.)$ , where  $m = \pm 1$ . Four typical scattering processes are plotted in Fig. 3, which are all the dominant scattering processes at incommensurate filling as we will discuss later.

The long wavelength physics or macroscopic properties of the system is dominated by low energy scattering processes near the Fermi points. These  $g$ -ology classified scattering processes serve as building blocks for the low energy effective theory. We can decouple the microscopic Hamiltonian in terms of these processes to obtain the effective theory.

For instance, the inter-band Hubbard repulsion interaction  $U'$  between two degenerate  $E'$  bands  $m = \pm 1$  can be decoupled as follows,

$$\begin{aligned} & U' \sum_{m\sigma\sigma'} c_{im\sigma}^\dagger c_{im\sigma} c_{i\bar{m}\sigma'}^\dagger c_{i\bar{m}\sigma'} \\ &= U' \sum_{pm\sigma} \left( \psi_{pm\sigma}^\dagger \psi_{\bar{p}\bar{m}\sigma}^\dagger \psi_{\bar{p}\bar{m}\sigma} \psi_{pm\sigma} + \psi_{pm\sigma}^\dagger \psi_{\bar{p}\bar{m}\sigma}^\dagger \psi_{\bar{p}\bar{m}\sigma} \psi_{pm\sigma} \right. \\ & \quad + \psi_{pm\sigma}^\dagger \psi_{\bar{p}\bar{m}\sigma}^\dagger \psi_{\bar{p}\bar{m}\sigma} \psi_{\bar{p}\bar{m}\sigma} + \psi_{pm\sigma}^\dagger \psi_{\bar{p}\bar{m}\sigma}^\dagger \psi_{\bar{p}\bar{m}\sigma} \psi_{pm\sigma} \\ & \quad + \psi_{pm\sigma}^\dagger \psi_{\bar{p}\bar{m}\sigma}^\dagger \psi_{\bar{p}\bar{m}\sigma} \psi_{\bar{p}\bar{m}\sigma} + \psi_{pm\sigma}^\dagger \psi_{\bar{p}\bar{m}\sigma}^\dagger \psi_{\bar{p}\bar{m}\sigma} \psi_{pm\sigma} \\ & \quad \left. + \psi_{pm\sigma}^\dagger \psi_{\bar{p}\bar{m}\sigma}^\dagger \psi_{\bar{p}\bar{m}\sigma} \psi_{\bar{p}\bar{m}\sigma} + \psi_{pm\sigma}^\dagger \psi_{\bar{p}\bar{m}\sigma}^\dagger \psi_{\bar{p}\bar{m}\sigma} \psi_{pm\sigma} \right). \quad (5) \end{aligned}$$

The initial values of the coupling constants ( $f$ 's and  $g$ 's) in the effective theory are determined by the microscopic Hamiltonian  $H^F$ . Decoupling all the terms in  $H_{int}^F$  in Eq. (1c) and collecting all the scattering processes, we obtain the values of nonzero coupling constants,

$$\begin{aligned} g_{1\perp}^{(1)} &= g_{1\perp}^{(2)} = g_{3\perp}^{(1)} = g_{3\perp}^{(2)} \\ &= f_{1\perp}^{(1)} = f_{1\perp}^{(2)} = f_{3\perp}^{(1)} = f_{3\perp}^{(2)} = J, \quad (6a) \end{aligned}$$

$$g_{4\perp}^{(1)} = g_{4\perp}^{(2)} = g_{\perp}^{(1)} = g_{\perp}^{(2)} = U, \quad (6b)$$

$$g_{2\perp}^{(1)} = g_{2\perp}^{(2)} = f_{2\perp}^{(1)} = f_{2\perp}^{(2)} = U - 2J, \quad (6c)$$

$$g_{2\parallel}^{(1)} = g_{2\parallel}^{(2)} = f_{2\parallel}^{(1)} = f_{2\parallel}^{(2)} = U - 3J, \quad (6d)$$

where the relations Eq. (2) and Eq. (3) have been used in deriving the above equations. Finally, we shall take the continuum limit by using Eq. (4) to obtain the fermion field theory.

TABLE I.  $g$ -ology for the three-band spinful fermion system.

| chirality    | band  |       |   | spin  |  |                  |   |
|--------------|---|-------|---|-------|--|------------------|---|
| $g(f)^{(1)}$ | $\psi_p^\dagger \psi_{\bar{p}}^\dagger \psi_p \psi_{\bar{p}}$ | $g_1$ | $\psi_m^\dagger \psi_{\bar{m}}^\dagger \psi_m \psi_{\bar{m}}$ | $f_1$ | $\psi_m^\dagger \psi_0^\dagger \psi_m \psi_0 + h.c.$ | $g(f)_\parallel$ | $\psi_\sigma^\dagger \psi_\sigma^\dagger \psi_\sigma \psi_\sigma$         |
| $g(f)^{(2)}$ | $\psi_p^\dagger \psi_{\bar{p}}^\dagger \psi_{\bar{p}} \psi_p$ | $g_2$ | $\psi_m^\dagger \psi_{\bar{m}}^\dagger \psi_{\bar{m}} \psi_m$ | $f_2$ | $\psi_m^\dagger \psi_0^\dagger \psi_0 \psi_m + h.c.$ | $g(f)_\perp$     | $\psi_\sigma^\dagger \psi_\sigma^\dagger \psi_{\bar{\sigma}} \psi_\sigma$ |
| $g(f)^{(3)}$ | $\psi_p^\dagger \psi_p^\dagger \psi_{\bar{p}} \psi_{\bar{p}}$ | $g_3$ | $\psi_m^\dagger \psi_m^\dagger \psi_{\bar{m}} \psi_{\bar{m}}$ | $f_3$ | $\psi_m^\dagger \psi_m^\dagger \psi_0 \psi_0 + h.c.$ |                  |   |
| $g(f)^{(4)}$ | $\psi_p^\dagger \psi_{\bar{p}}^\dagger \psi_p \psi_p$         | $g_4$ | $\psi_m^\dagger \psi_{\bar{m}}^\dagger \psi_m \psi_m$         | $g$   | $\psi_0^\dagger \psi_0^\dagger \psi_0 \psi_0$        |                  |   |

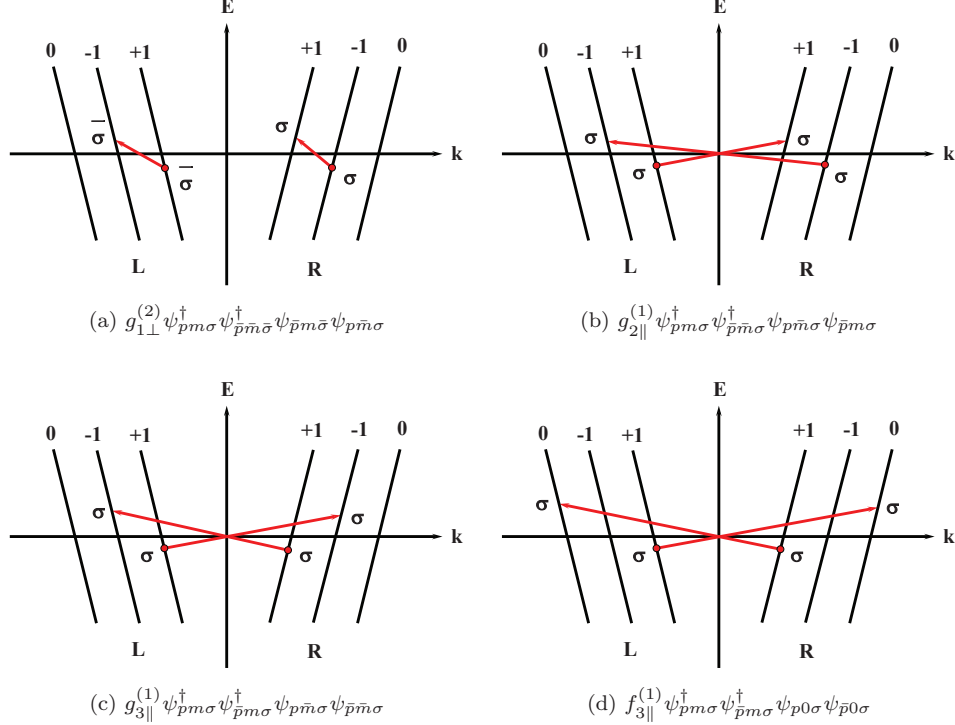


FIG. 3. Four dominant scattering processes at incommensurate filling: (a)  $g_{1\perp}^{(2)} \psi_{pm\sigma}^\dagger \psi_{\bar{p}\bar{m}\bar{\sigma}}^\dagger \psi_{\bar{p}\bar{m}\bar{\sigma}} \psi_{p\bar{m}\sigma}$ , (b)  $g_{2\parallel}^{(1)} \psi_{pm\sigma}^\dagger \psi_{\bar{p}\bar{m}\sigma}^\dagger \psi_{p\bar{m}\sigma} \psi_{\bar{p}\bar{m}\sigma}$ , (c)  $g_{3\parallel}^{(1)} \psi_{pm\sigma}^\dagger \psi_{\bar{p}\bar{m}\sigma}^\dagger \psi_{p\bar{m}\sigma} \psi_{\bar{p}\bar{m}\sigma}$  and (d)  $f_{3\parallel}^{(1)} \psi_{pm\sigma}^\dagger \psi_{\bar{p}\bar{m}\sigma}^\dagger \psi_{p0\sigma} \psi_{\bar{p}0\sigma}$ .

#### IV. BOSONIZATION

To study low energy effective theory, we shall utilize the standard bosonization technique to analyze the continuum fermion model. In abelian bosonization, the fermion operators can be expressed in terms of boson operators as follows<sup>23</sup>,

$$\psi_{pm\sigma} = \frac{\eta_{m\sigma}}{\sqrt{2\pi a}} e^{ipk_{Fm}x} e^{-ip\varphi_{pm\sigma}}, \quad (7a)$$

where  $k_{Fm}$  is the Fermi momentum for band  $m$ ,  $a$  is the cutoff which can be chosen as the lattice constant, and  $p = 1(-1)$  stands for  $R(L)$  branch. The Klein factors  $\eta_{m\sigma}$  ensure the fermionic statistics and obey the anti-commutation relations

$$\{\eta_{m\sigma}, \eta_{m'\sigma'}\} = 2\delta_{mm'}\delta_{\sigma\sigma'}. \quad (7b)$$

Counting the four-fermion interactions, there are still some gauge degrees of freedom for choosing the values of product of two Klein factors with different band indices  $m$ . In this paper, we adopt the convention

$$\eta_{m\sigma}\eta_{\bar{m}\sigma} = \eta_{0\sigma}\eta_{m\sigma} = im\sigma, \quad (7c)$$

$$\eta_{m\sigma}\eta_{m\bar{\sigma}} = \eta_{0\sigma}\eta_{0\bar{\sigma}} = i\sigma, \quad (7d)$$

$$\eta_{m\sigma}\eta_{\bar{m}\bar{\sigma}} = \eta_{0\sigma}\eta_{m\bar{\sigma}} = im, \quad (7e)$$

where  $m = \pm 1$  and  $\sigma = +1(-1)$  for spin up(down). As we will see later in this section, these products of two Klein factors will determine the sign of coupling constants in the bosonic interacting Hamiltonian.

The chiral fields  $\varphi_{pm\sigma}$  can be written in terms of two non-chiral fields  $\phi_{m\sigma}$  and  $\theta_{m\sigma}$  through

$$\varphi_{pm\sigma} = \phi_{m\sigma} - p\theta_{m\sigma}. \quad (7f)$$

Their gradients are proportional to fermionic density and current operator respectively,

$$\nabla\phi_{m\sigma} \propto n_{m\sigma} = \psi_{Rm\sigma}^\dagger \psi_{Rm\sigma} + \psi_{Lm\sigma}^\dagger \psi_{Lm\sigma}, \quad (7g)$$

$$\nabla\theta_{m\sigma} \propto j_{m\sigma} = \psi_{Rm\sigma}^\dagger \psi_{Rm\sigma} - \psi_{Lm\sigma}^\dagger \psi_{Lm\sigma}. \quad (7h)$$

Thus the four-fermion density-density and current-current interaction can be bosonized into quadratic terms in the bosonic Hamiltonian.

Furthermore, the fields  $\phi_{m\sigma}$  and  $\theta_{m\sigma}$  can be decomposed into their charge and spin degrees of freedom,

$$\phi_{m\sigma} = \frac{1}{\sqrt{2}} (\phi_{cm} + \sigma\phi_{sm}), \quad (7i)$$

$$\theta_{m\sigma} = \frac{1}{\sqrt{2}} (\theta_{cm} + \sigma\theta_{sm}). \quad (7j)$$

Since both charge and spin are conserved,  $\phi_{cm}(\theta_{cm})$  and  $\phi_{sm}(\theta_{sm})$  can be diagonalized separately in the quadratic part of the bosonic Hamiltonian  $H_0^B$ . The diagonalization can be done explicitly by the following transformation,

$$\begin{pmatrix} \phi(\theta)_{\mu+1} \\ \phi(\theta)_{\mu-1} \\ \phi(\theta)_{\mu 0} \end{pmatrix} = \begin{pmatrix} \frac{1}{\sqrt{2}} & \frac{1}{\sqrt{6}} & \frac{1}{\sqrt{3}} \\ -\frac{1}{\sqrt{2}} & \frac{1}{\sqrt{6}} & \frac{1}{\sqrt{3}} \\ 0 & -\frac{2}{\sqrt{6}} & \frac{1}{\sqrt{3}} \end{pmatrix} \begin{pmatrix} \tilde{\phi}(\tilde{\theta})_{\mu+1} \\ \tilde{\phi}(\tilde{\theta})_{\mu-1} \\ \tilde{\phi}(\tilde{\theta})_{\mu 0} \end{pmatrix}, \quad (8)$$

where  $\mu = c, s$  refers to charge and spin components.

Near the Fermi points, the energy dispersion  $\xi_{km}$  can be linearized as

$$\xi_{km} = v_{Fm} (k - k_{Fm}), \quad (9)$$

where  $v_{Fm}$  is the Fermi velocity and  $k_{Fm}$  is the Fermi momentum. According to the DFT calculation, the difference between  $v_{F0}$  and  $v_{F\pm 1}$  is small. On the other hand, we will show below that forward scatterings will renormalize the Fermi velocities. Thus this small difference is inessential and we assume  $v_{F0} = v_{F\pm 1} = v_F$  at first.

The bosonized Hamiltonian  $H^B$  also contain two parts,

$$H^B = H_0^B + H_{int}^B. \quad (10)$$

$H_0^B$  is the quadratic or non-interacting part, and  $H_{int}^B$  is the interacting part. The non-interacting part  $H_0^B$  can be diagonalized by Eq. (8), resulting in

$$H_0^B = \frac{1}{2\pi} \int dx \sum_{\mu\nu} v_{\mu\nu} \left[ K_{\mu\nu} (\nabla\tilde{\theta}_{\mu\nu})^2 + \frac{1}{K_{\mu\nu}} (\nabla\tilde{\phi}_{\mu\nu})^2 \right] \quad (11)$$

where  $\mu = c, s$  and  $\nu = 0, \pm 1$ . The renormalized Fermi velocities  $v_{\mu\nu}$  and Luttinger parameters  $K_{\mu\nu}$  are given by

$$\frac{v_{c(s)\pm 1}}{v_F} = \sqrt{1 - \frac{\left[ +(-)g_{4\perp}^{(2)} - (g_{2\parallel}^{(2)} + (-)g_{2\perp}^{(2)}) \right]^2}{(2\pi v_F)^2}}, \quad (12a)$$

$$\frac{v_{c(s)0}}{v_F} = \sqrt{1 - \frac{\left[ +(-)g_{4\perp}^{(2)} + 2(g_{2\parallel}^{(2)} + (-)g_{2\perp}^{(2)}) \right]^2}{(2\pi v_F)^2}}, \quad (12b)$$

$$K_{c(s)\pm 1} = \sqrt{\frac{1 - \frac{1}{2\pi v_F} \left[ +(-)g_{4\perp}^{(2)} - (g_{2\parallel}^{(2)} + (-)g_{2\perp}^{(2)}) \right]}{1 + \frac{1}{2\pi v_F} \left[ +(-)g_{4\perp}^{(2)} - (g_{2\parallel}^{(2)} + (-)g_{2\perp}^{(2)}) \right]}}, \quad (12c)$$

$$K_{c(s)0} = \sqrt{\frac{1 - \frac{1}{2\pi v_F} \left[ +(-)g_{4\perp}^{(2)} + 2(g_{2\parallel}^{(2)} + (-)g_{2\perp}^{(2)}) \right]}{1 + \frac{1}{2\pi v_F} \left[ +(-)g_{4\perp}^{(2)} + 2(g_{2\parallel}^{(2)} + (-)g_{2\perp}^{(2)}) \right]}}. \quad (12d)$$

The spin-charge separation is reflected in  $v_{cm} \neq v_{sm}$ , which is similar to single band Luttinger liquids. The difference between single-band and three-band model is the following. For the single-band model, all the forward scattering processes contribute to the bosonic non-interacting Hamiltonian  $H_0^B$ . However, for the three-band model, some  $g^{(2)}$  forward scattering processes contribute to the interacting part  $H_{int}^B$  but not the non-interacting part  $H_0^B$ , which can be seen in Eq. (13) below. This difference is due to the fact that there is only partial forward scattering processes that can be expressed in the form of density-density or current-current interaction, renormalizing the Luttinger parameters  $K_{\mu\nu}$ .

Note that we have omitted the coupling constants with zero initial values in the derivation of  $H_0^B$ . These coupling constants do not flow under the renormalization group (RG) transformation. We have also dropped all the  $g^{(3)}$  umklapp scattering processes, which is negligible when the fermion system is away from half-filling. All the  $g^{(4)}$  and  $f^{(4)}$  scattering processes happen within the same chirality and have small momentum transfer. These small-momentum-transfer terms is irrelevant in the sense of RG. In fact, the  $g^{(4)}$  terms will renormalize both  $v_{\mu\nu}$  and  $K_{\mu\nu}$ . However, if one expands  $v_{\mu\nu}$  and  $K_{\mu\nu}$  in power of  $g^{(4)}$ , the first order terms will vanish. So that we can safely neglect  $g^{(4)}$  and  $f^{(4)}$  in both  $H_0^B$  and  $H_{int}^B$  in perturbation RG, which will not change the conclusions of our perturbation RG analysis in remaining parts of this paper.

The bosonic interacting Hamiltonian  $H_{int}^B$  is given by

$$\begin{aligned}
H_{int}^B = & -g_{1\perp}^{(1)} \frac{4}{(2\pi a)^2} \int dx \cos\left(\frac{2}{\sqrt{3}}\tilde{\phi}_{s-1} + \frac{4}{\sqrt{6}}\tilde{\phi}_{s0}\right) \cos\left(2\tilde{\theta}_{s+1}\right) \\
& + g_{2\parallel}^{(1)} \frac{4}{(2\pi a)^2} \int dx \cos\left(2\tilde{\phi}_{c+1}\right) \cos\left(2\tilde{\phi}_{s+1}\right) \\
& + g_{2\perp}^{(1)} \frac{4}{(2\pi a)^2} \int dx \cos\left(2\tilde{\phi}_{c+1}\right) \cos\left(\frac{2}{\sqrt{3}}\tilde{\phi}_{s-1} + \frac{4}{\sqrt{6}}\tilde{\phi}_{s0}\right) \\
& + g_{3\parallel}^{(1)} \frac{4}{(2\pi a)^2} \int dx \cos\left(2\tilde{\theta}_{c+1}\right) \cos\left(2\tilde{\theta}_{s+1}\right) \\
& + g_{3\perp}^{(1)} \frac{4}{(2\pi a)^2} \int dx \cos\left(2\tilde{\theta}_{c+1}\right) \cos\left(\frac{2}{\sqrt{3}}\tilde{\phi}_{s-1} + \frac{4}{\sqrt{6}}\tilde{\phi}_{s0}\right) \\
& + g_{4\perp}^{(1)} \frac{4}{(2\pi a)^2} \int dx \cos\left(2\tilde{\phi}_{s+1}\right) \cos\left(\frac{2}{\sqrt{3}}\tilde{\phi}_{s-1} + \frac{4}{\sqrt{6}}\tilde{\phi}_{s0}\right) \\
& - g_{1\perp}^{(2)} \frac{4}{(2\pi a)^2} \int dx \cos\left(2\tilde{\phi}_{c+1}\right) \cos\left(2\tilde{\theta}_{s+1}\right) \\
& + g_{3\perp}^{(2)} \frac{4}{(2\pi a)^2} \int dx \cos\left(2\tilde{\theta}_{c+1}\right) \cos\left(2\tilde{\phi}_{s+1}\right) \\
& - f_{1\perp}^{(1)} \frac{8}{(2\pi a)^2} \int dx \left[ \cos\tilde{\phi}_{s+1} \cos\left(-\frac{1}{\sqrt{3}}\tilde{\phi}_{s-1} + \frac{4}{\sqrt{6}}\tilde{\phi}_{s0}\right) \cos\tilde{\theta}_{s+1} \cos\sqrt{3}\tilde{\theta}_{s-1} + (\cos \rightarrow \sin) \right] \\
& + f_{3\parallel}^{(1)} \frac{8}{(2\pi a)^2} \int dx \left[ \cos\tilde{\theta}_{c+1} \cos\sqrt{3}\tilde{\theta}_{c-1} \cos\tilde{\theta}_{s+1} \cos\sqrt{3}\tilde{\theta}_{s-1} + (\cos \rightarrow \sin) \right] \\
& + f_{3\perp}^{(1)} \frac{8}{(2\pi a)^2} \int dx \left[ \cos\tilde{\theta}_{c+1} \cos\sqrt{3}\tilde{\theta}_{c-1} \cos\tilde{\phi}_{s+1} \cos\left(-\frac{1}{\sqrt{3}}\tilde{\phi}_{s-1} + \frac{4}{\sqrt{6}}\tilde{\phi}_{s0}\right) + (\cos \rightarrow \sin) \right] \\
& + f_{3\perp}^{(2)} \frac{8}{(2\pi a)^2} \int dx \left[ \cos\tilde{\theta}_{c+1} \cos\sqrt{3}\tilde{\theta}_{c-1} \cos\tilde{\phi}_{s+1} \cos\sqrt{3}\tilde{\phi}_{s-1} + (\cos \rightarrow \sin) \right] \\
& + g_{\perp}^{(1)} \frac{2}{(2\pi a)^2} \int dx \cos\left(-\frac{4}{\sqrt{3}}\tilde{\phi}_{s-1} + \frac{4}{\sqrt{6}}\tilde{\phi}_{s0}\right). \tag{13}
\end{aligned}$$

Unlike the non-interacting situation in  $H_0^B$ , here we retain the terms with zero initial values of coupling constants in  $H_{int}^B$ , namely,  $g_{3\parallel}^{(1)}$  and  $f_{3\parallel}^{(1)}$ . These terms will be automatically generated in the one-loop RG to form the closed algebra of operator product expansion (OPE). Since different scattering processes may give rise to the same form in the bosonized Hamiltonian, we have incorporated them into a single term, e.g.  $g_{3\parallel}^{(1)}$  and  $g_{3\parallel}^{(2)}$  terms. As mentioned before, both forward scattering and back scattering processes will contribute to  $H_{int}^B$ , which is different from the single-band case.

The non-interacting Hamiltonian  $H_0^B$  describes a three-band Luttinger liquid, which is a Gaussian fixed point under RG transformation. In the remaining sections, we shall treat the interacting part  $H_{int}^B$  as a perturbation and perform RG analysis to investigate its relevance. The (most) relevant terms in  $H_{int}^B$  will give the low energy effective field theories. In such effective field theories, the fields  $\phi_{\mu\nu}$  and  $\theta_{\mu\nu}$  will be locked around some saddle points, say, the extrema of cosine functions in Eq. (13), which gives rise to some ordered states or relevant instabilities. To classify such orders or insta-

bilites, we shall introduce order parameters in the next section at first.

## V. ORDER PARAMETER

To characterize different effective field theories in low energies, we shall introduce order parameters in this section. In general, the order parameter can be defined as fermionic bilinear, or more precisely, long-ranged correlation of bilinear fermionic operators. By this definition, there are two classes of order parameters in such a three-band system. One is defined in the particle-hole channels,

$$O_{ph}^{ij} = \sum_{mm'\sigma\sigma'} \lambda_{mm'}^i \tau_{\sigma\sigma'}^j \psi_{Rm\sigma}^\dagger \psi_{Lm'\sigma'}, \tag{14a}$$

and the other is defined in particle-particle channels (or their Hermitian conjugates in hole-hole channels),

$$O_{pp}^{ij} = \sum_{mm'\sigma\sigma'} \sigma \lambda_{mm'}^i \tau_{\sigma\sigma'}^j \psi_{Rm\sigma}^\dagger \psi_{Lm'\bar{\sigma}}. \tag{14b}$$

Here  $\lambda^i (i = 1, \dots, 8)$  are Gell-Mann matrices,  $\tau^j (j = 1, 2, 3)$  are Pauli matrices. We have also defined  $\lambda^0$  and  $\sigma^0$  as  $3 \times 3$  and  $2 \times 2$  unit matrices respectively.  $\psi_{pm\sigma} (\psi_{pm\sigma}^\dagger)$  is the electron annihilation (creation) operator with chirality  $p$ , band  $m$  and spin  $\sigma$ .

Note that we only keep opposite-chirality terms,  $\psi_R^\dagger \psi_L$  and  $\psi_R^\dagger \psi_L^\dagger$  in Eq. (14) and ignore equal-chirality terms, such as  $\psi_R^\dagger \psi_R$ ,  $\psi_L^\dagger \psi_L$ ,  $\psi_R^\dagger \psi_R^\dagger$ , and  $\psi_L^\dagger \psi_L^\dagger$ . This is because four-fermion operators in the same chirality, e.g.  $\psi_R^\dagger \psi_R^\dagger \psi_R^\dagger \psi_R$  and  $\psi_R^\dagger \psi_R \psi_R^\dagger \psi_R$  are all irrelevant in the sense of RG. Physically, all our familiar ordered states, including charge density wave (CDW), spin density wave

(SDW), and superconducting (SC) states, arise from scattering or pairing in opposite chiralities. So that Eq. (14) contains all possible physically relevant order parameters constructed by fermionic bilinears.

We shall identify physical ordered states for each order parameters in Eq. (14) and bosonize them. For particle-hole channels, we find that  $O_{ph}^{i0}$  refers to CDW and  $O_{ph}^{i1-3}$  refer to three components of SDW. There are total  $9 \times 4 = 36$  order parameters in particle-hole channels. Below we only list 4  $\lambda^1$ -components as examples, which involve only two  $E'$  bands with  $m = \pm 1$ . After bosonization, these four order parameters read

$$O_{ph}^{10} \propto e^{-i2k_F x + i\left(\frac{1}{\sqrt{3}}\tilde{\phi}_{c-1} + \frac{2}{\sqrt{6}}\tilde{\phi}_{c0}\right)} \left[ \cos\left(\frac{1}{\sqrt{3}}\tilde{\phi}_{s-1} + \frac{2}{\sqrt{6}}\tilde{\phi}_{s0}\right) \cos\tilde{\theta}_{c+1} \sin\tilde{\theta}_{s+1} + i(\cos \leftrightarrow \sin) \right], \quad (15a)$$

$$O_{ph}^{11} \propto e^{-i2k_F x + i\left(\frac{1}{\sqrt{3}}\tilde{\phi}_{c-1} + \frac{2}{\sqrt{6}}\tilde{\phi}_{c0}\right)} \left[ \cos\left(\frac{1}{\sqrt{3}}\tilde{\theta}_{s-1} + \frac{2}{\sqrt{6}}\tilde{\theta}_{s0}\right) \sin\tilde{\theta}_{c+1} \cos\tilde{\phi}_{s+1} + i(\cos \leftrightarrow \sin) \right], \quad (15b)$$

$$O_{ph}^{12} \propto e^{-i2k_F x + i\left(\frac{1}{\sqrt{3}}\tilde{\phi}_{c-1} + \frac{2}{\sqrt{6}}\tilde{\phi}_{c0}\right)} \left[ \sin\left(\frac{1}{\sqrt{3}}\tilde{\theta}_{s-1} + \frac{2}{\sqrt{6}}\tilde{\theta}_{s0}\right) \sin\tilde{\theta}_{c+1} \cos\tilde{\phi}_{s+1} - i(\cos \leftrightarrow \sin) \right], \quad (15c)$$

$$O_{ph}^{13} \propto e^{-i2k_F x + i\left(\frac{1}{\sqrt{3}}\tilde{\phi}_{c-1} + \frac{2}{\sqrt{6}}\tilde{\phi}_{c0}\right)} \left[ \cos\left(\frac{1}{\sqrt{3}}\tilde{\phi}_{s-1} + \frac{2}{\sqrt{6}}\tilde{\phi}_{s0}\right) \sin\tilde{\theta}_{c+1} \cos\tilde{\theta}_{s+1} + i(\cos \leftrightarrow \sin) \right], \quad (15d)$$

where  $2k_F = k_{F+1} + k_{F-1}$ , and  $(\cos \leftrightarrow \sin)$  means replacing all the cosine functions by sine functions and vice versa.

For particle-particle channels, we find that  $O_{pp}^{i0}$  serves

as singlet superconducting (SSC) pairing order parameter and  $O_{pp}^{i1-3}$  serve as three components of triplet superconducting (TSC) pairing order parameters. The bosonization for  $\lambda^2$ -components is the following,

$$O_{pp}^{20} \propto e^{i\left(\frac{1}{\sqrt{3}}\tilde{\theta}_{c-1} + \frac{2}{\sqrt{6}}\tilde{\theta}_{c0}\right)} \left[ \cos\left(\frac{1}{\sqrt{3}}\tilde{\phi}_{s-1} + \frac{2}{\sqrt{6}}\tilde{\phi}_{s0}\right) \sin\tilde{\phi}_{c+1} \sin\tilde{\theta}_{s+1} - i(\cos \leftrightarrow \sin) \right], \quad (16a)$$

$$O_{pp}^{21} \propto e^{i\left(\frac{1}{\sqrt{3}}\tilde{\theta}_{c-1} + \frac{2}{\sqrt{6}}\tilde{\theta}_{c0}\right)} \left[ \cos\left(\frac{1}{\sqrt{3}}\tilde{\theta}_{s-1} + \frac{2}{\sqrt{6}}\tilde{\theta}_{s0}\right) \cos\tilde{\phi}_{c+1} \cos\tilde{\phi}_{s+1} - i(\cos \leftrightarrow \sin) \right], \quad (16b)$$

$$O_{pp}^{22} \propto e^{i\left(\frac{1}{\sqrt{3}}\tilde{\theta}_{c-1} + \frac{2}{\sqrt{6}}\tilde{\theta}_{c0}\right)} \left[ \sin\left(\frac{1}{\sqrt{3}}\tilde{\theta}_{s-1} + \frac{2}{\sqrt{6}}\tilde{\theta}_{s0}\right) \cos\tilde{\phi}_{c+1} \cos\tilde{\phi}_{s+1} + i(\cos \leftrightarrow \sin) \right], \quad (16c)$$

$$O_{pp}^{23} \propto e^{i\left(\frac{1}{\sqrt{3}}\tilde{\theta}_{c-1} + \frac{2}{\sqrt{6}}\tilde{\theta}_{c0}\right)} \left[ \cos\left(\frac{1}{\sqrt{3}}\tilde{\phi}_{s-1} + \frac{2}{\sqrt{6}}\tilde{\phi}_{s0}\right) \cos\tilde{\phi}_{c+1} \cos\tilde{\theta}_{s+1} - i(\cos \leftrightarrow \sin) \right]. \quad (16d)$$

Each bosonized order parameter contains two parts, which are related to each other by interchanging  $\cos \leftrightarrow \sin$ . If one shifts the bosonic fields  $\theta_{\mu+1}$  and  $\phi_{\mu+1}$  by  $\frac{\pi}{\sqrt{2}}$ ,

$$\phi(\theta)_{\mu+1} \rightarrow \phi(\theta)_{\mu+1} + \frac{\pi}{\sqrt{2}}, \quad (17)$$

while leaves other  $\theta_{\mu\nu}$ 's and  $\phi_{\mu\nu}$ 's unchanged, the digo-

nalized fields  $\tilde{\theta}_{\mu\nu}$  and  $\tilde{\phi}_{\mu\nu}$  will transfer accordingly,

$$\begin{aligned} \tilde{\phi}(\tilde{\theta})_{\mu+1} &\rightarrow \tilde{\phi}(\tilde{\theta})_{\mu+1} + \frac{\pi}{2}, \\ \tilde{\phi}(\tilde{\theta})_{\mu-1} &\rightarrow \tilde{\phi}(\tilde{\theta})_{\mu-1} + \frac{\pi}{2\sqrt{3}}, \\ \tilde{\phi}(\tilde{\theta})_{\mu 0} &\rightarrow \tilde{\phi}(\tilde{\theta})_{\mu 0} + \frac{\pi}{\sqrt{6}}. \end{aligned}$$

So that

$$\frac{1}{\sqrt{3}}\tilde{\phi}(\tilde{\theta})_{\mu-1} + \frac{2}{\sqrt{6}}\tilde{\phi}(\tilde{\theta})_{\mu 0} \rightarrow \frac{1}{\sqrt{3}}\tilde{\phi}(\tilde{\theta})_{\mu-1} + \frac{2}{\sqrt{6}}\tilde{\phi}(\tilde{\theta})_{\mu 0} + \frac{\pi}{2}.$$

It means that the order parameters  $O_{ph}^{i1-3}$  and  $O_{pp}^{i1-3}$  will not change under the phase shift given in Eq. (17). This can be verified by the bosonization formula Eq. (7) too.

In the following RG analysis, the coupling constants will flow to zero if irrelevant and to strong coupling limit if relevant. The relevant coupling constants will lock the corresponding bosonic fields  $\theta_{\mu\nu}$  and  $\phi_{\mu\nu}$  around the saddle points, say, in the extremum of cosine or sine functions to minimize the action. If we substitute these saddle-point values of bosonic fields into the order parameters, we will obtain the nonzero order parameters. For instance, the saddle point

$$\left( \frac{1}{\sqrt{3}}\tilde{\phi}_{s-1} + \frac{2}{\sqrt{6}}\tilde{\phi}_{s0}, \tilde{\phi}_{c+1}, \tilde{\theta}_{s+1} \right) = (0, 0, 0) \quad (18)$$

will give rise to nonzero amplitude for order parameter  $O_{pp}^{23}$  in Eq. (16). The remaining phase factor

$$e^i \left( \frac{1}{\sqrt{3}}\tilde{\theta}_{c-1} + \frac{2}{\sqrt{6}}\tilde{\theta}_{c0} \right) = e^{\frac{i}{\sqrt{2}}(\theta_{c+1} + \theta_{c-1})}$$

reflects the  $U(1)$  gauge symmetry, which will spontaneously break when the superconducting long ranged order is established.

## VI. RENORMALIZATION-GROUP ANALYSIS

The quadratic part of the Hamiltonian,  $H_0^B$ , is a well defined Gaussian fixed point under renormalization group, describing the three-band Tomonaga-Luttinger liquids at high temperatures, which serves a good start point for our study. In this section, we begin with the quadratic (non-interacting) part  $H_0^B$  and treat the non-quadratic (interacting) part  $H_{int}^B$  by a RG method perturbatively. We shall use operator product expansion (OPE) method<sup>24</sup> to derive the RG equations for the 13 coupling constants in Eq. (13) up to one loop.

The general form of one-loop perturbative RG equations read

$$\frac{dg_k}{dl} = (d - \Delta_k)g_k - \sum_{ij} C_{ij}^k g_i g_j, \quad (19)$$

where  $g_k$  represents the coupling constants ( $g$ 's and  $f$ 's) in  $H_{int}^B$  in Eq. (13). The linear term in Eq. (19) is the tree-level contribution and depends on space-time dimension  $d$  and scaling dimension  $\Delta_k$ . The quadratic terms are the one-loop contributions. The coefficients  $C_{ij}^k$  are the structure constants of the OPE, which can be obtained by the fusion of arbitrary two terms in  $H_{int}^B$ . This process will generate new terms, which are absent in the original microscopic Hamiltonian, until all terms form a closed algebra. This is the reason why we retain the terms with zero initial values of coupling constants in Eq. (13).

In the spirit of perturbation theory, we shall firstly derive and analyze RG equations at tree-level, and then carry out one-loop analysis in the remaining parts of this section.

### VI.1. Tree-level RG

To simplify, we introduce the renormalized coupling constants

$$y_i = \frac{g_i}{\pi v_F}, \quad (20a)$$

$$x_i = \frac{f_i}{\pi v_F}. \quad (20b)$$

As shown in Appendix A, the tree-level RG equations in weak coupling can be written in terms of  $x_i$  and  $y_i$ 's,

$$\frac{dy_{1\perp}^{(1)}}{dl} = \left( y_{2\parallel}^{(2)} - y_{2\perp}^{(2)} \right) y_{1\perp}^{(1)}, \quad (21a)$$

$$\frac{dy_{2\parallel}^{(1)}}{dl} = -y_{2\parallel}^{(2)} y_{2\parallel}^{(1)}, \quad (21b)$$

$$\frac{dy_{2\perp}^{(1)}}{dl} = -y_{2\perp}^{(2)} y_{2\perp}^{(1)}, \quad (21c)$$

$$\frac{dy_{3\parallel}^{(1)}}{dl} = y_{2\parallel}^{(2)} y_{3\parallel}^{(1)}, \quad (21d)$$

$$\frac{dy_{3\perp}^{(1)}}{dl} = \left( -y_{4\perp}^{(2)} + y_{2\parallel}^{(2)} \right) y_{3\perp}^{(1)}, \quad (21e)$$

$$\frac{dy_{4\perp}^{(1)}}{dl} = -y_{2\perp}^{(2)} y_{4\perp}^{(1)}, \quad (21f)$$

$$\frac{dy_{1\perp}^{(2)}}{dl} = \left( y_{4\perp}^{(2)} - y_{2\perp}^{(2)} \right) y_{1\perp}^{(2)}, \quad (21g)$$

$$\frac{dy_{3\perp}^{(2)}}{dl} = \left( -y_{4\perp}^{(2)} + y_{2\perp}^{(2)} \right) y_{3\perp}^{(2)}, \quad (21h)$$

$$\frac{dx_{1\perp}^{(1)}}{dl} = \left( y_{2\parallel}^{(2)} - y_{2\perp}^{(2)} \right) x_{1\perp}^{(1)}, \quad (21i)$$

$$\frac{dx_{3\parallel}^{(1)}}{dl} = y_{2\parallel}^{(2)} x_{3\parallel}^{(1)}, \quad (21j)$$

$$\frac{dx_{3\perp}^{(1)}}{dl} = \left( -y_{4\perp}^{(2)} + y_{2\parallel}^{(2)} \right) x_{3\perp}^{(1)}, \quad (21k)$$

$$\frac{dx_{3\perp}^{(2)}}{dl} = \left( -y_{4\perp}^{(2)} + y_{2\perp}^{(2)} \right) x_{3\perp}^{(2)}, \quad (21l)$$



$$\frac{dy_{\perp}^{(1)}}{dl} = -y_{4\perp}^{(2)}y_{\perp}^{(1)}. \quad (21m)$$

In the formulation of Abelian bosonization, Eqs. (7), the variables  $y_{2\parallel}^{(2)}$ ,  $y_{2\perp}^{(2)}$  and  $y_{4\perp}^{(2)}$  in Eqs. (A3) and (21) only appear in the quadratic part  $H_0^B$  in the original microscopic Hamiltonian, thus do not flow under the RG transformation. So that we use their initial values  $y_{2\parallel}^{(2)} = \frac{U-3J}{\pi v_F}$ ,  $y_{2\perp}^{(2)} = \frac{U-2J}{\pi v_F}$  and  $y_{4\perp}^{(2)} = \frac{U}{\pi v_F}$  in tree-level analysis. However, this formulation does not conserve spin rotational symmetry. We shall discuss how to restore spin  $SU(2)$  symmetry in the next subsection, where  $y_{2\parallel}^{(2)}$ ,  $y_{2\perp}^{(2)}$  and  $y_{4\perp}^{(2)}$  can be expressed in terms of the 13 coupling constants in Eq. (13) and make the RG equations close.

The slope  $\{\frac{1}{x_i} \frac{dx_i}{dl}, \frac{1}{y_i} \frac{dy_i}{dl}\}$  around the Luttinger liquid fixed point will determine which coupling constants are relevant. In weak coupling, this slope is given by the initial values of the coupling constants in Eq. (6), say, the microscopic Hamiltonian with two parameters  $U > 0$  and  $J > 0$ . We find that there exist three parameters regions. (1) For  $0 < J < U/3$ , the coupling constants  $x_{3\parallel}^{(1)}$ ,  $y_{3\parallel}^{(1)}$  and  $y_{1\perp}^{(2)}$  are relevant, other coupling constants are irrelevant. (2) For  $U/3 < J < U/2$ , there are only two relevant coupling constants,  $y_{2\parallel}^{(1)}$  and  $y_{1\perp}^{(2)}$ . (3) For the unphysical region  $J > U/2$ , there are four relevant coupling constants,  $y_{2\parallel}^{(1)}$ ,  $y_{2\perp}^{(1)}$ ,  $y_{4\perp}^{(1)}$  and  $y_{1\perp}^{(2)}$ . However, the above analysis largely relies on tree-level RG equations. We should proceed to one-loop RG equations for further studies.

## VI.2. One-loop RG

With the help of spin  $SU(2)$  symmetry and the microscopic Hamiltonian, we are able to derive one-loop RG equations (see Appendix B) as follows,

$$\frac{dy_{1\perp}^{(1)}}{dl} = -\left(y_{1\perp}^{(1)}\right)^2 - y_{2\perp}^{(1)}y_{1\perp}^{(2)} + y_{3\parallel}^{(1)}y_{3\perp}^{(1)}, \quad (22a)$$

$$\frac{dy_{2\parallel}^{(1)}}{dl} = \frac{1}{2}y_{1\perp}^{(1)}y_{2\parallel}^{(1)} - y_{2\perp}^{(1)}y_{4\perp}^{(1)}, \quad (22b)$$

$$\frac{dy_{2\perp}^{(1)}}{dl} = -\frac{1}{2}y_{1\perp}^{(1)}y_{2\perp}^{(1)} - y_{1\perp}^{(1)}y_{1\perp}^{(2)} - y_{2\parallel}^{(1)}y_{4\perp}^{(1)}, \quad (22c)$$

$$\frac{dy_{3\parallel}^{(1)}}{dl} = -\frac{1}{2}y_{1\perp}^{(1)}y_{3\parallel}^{(1)} + y_{1\perp}^{(1)}y_{3\perp}^{(1)}, \quad (22d)$$

$$\begin{aligned} \frac{dy_{3\perp}^{(1)}}{dl} = & -\left(y_{4\perp}^{(1)} + \frac{1}{2}y_{1\perp}^{(1)}\right)y_{3\perp}^{(1)} + y_{1\perp}^{(1)}y_{3\parallel}^{(1)} \\ & - y_{4\perp}^{(1)}y_{3\perp}^{(2)}, \end{aligned} \quad (22e)$$

$$\frac{dy_{4\perp}^{(1)}}{dl} = \frac{1}{2}y_{1\perp}^{(1)}y_{4\perp}^{(1)} - y_{2\parallel}^{(1)}y_{2\perp}^{(1)} - y_{3\perp}^{(1)}y_{3\perp}^{(2)}, \quad (22f)$$

$$\frac{dy_{1\perp}^{(2)}}{dl} = \left(y_{4\perp}^{(1)} - \frac{1}{2}y_{1\perp}^{(1)}\right)y_{1\perp}^{(2)} - y_{1\perp}^{(1)}y_{2\perp}^{(1)}, \quad (22g)$$

$$\frac{dy_{3\perp}^{(2)}}{dl} = \left(-y_{4\perp}^{(1)} + \frac{1}{2}y_{1\perp}^{(1)}\right)y_{3\perp}^{(2)} - y_{3\perp}^{(1)}y_{4\perp}^{(1)}, \quad (22h)$$

$$\frac{dx_{1\perp}^{(1)}}{dl} = -\left(x_{1\perp}^{(1)}\right)^2 + x_{3\parallel}^{(1)}x_{3\perp}^{(1)}, \quad (22i)$$

$$\frac{dx_{3\parallel}^{(1)}}{dl} = -\frac{1}{2}x_{1\perp}^{(1)}x_{3\parallel}^{(1)} + x_{1\perp}^{(1)}x_{3\perp}^{(1)}, \quad (22j)$$

$$\frac{dx_{3\perp}^{(1)}}{dl} = -\left(y_{\perp}^{(1)} + \frac{1}{2}x_{1\perp}^{(1)}\right)x_{3\perp}^{(1)} + x_{1\perp}^{(1)}x_{3\parallel}^{(1)}, \quad (22k)$$

$$\frac{dx_{3\perp}^{(2)}}{dl} = \left(-y_{\perp}^{(1)} + \frac{1}{2}x_{1\perp}^{(1)}\right)x_{3\perp}^{(2)}, \quad (22l)$$

$$\frac{dy_{\perp}^{(1)}}{dl} = -\left(y_{\perp}^{(1)}\right)^2. \quad (22m)$$

The key to analyze these one-loop RG equations is to find fixed points, where the coupling constants will no longer flow under RG transformation<sup>25</sup>. We rewrite the RG equations in vector form

$$\frac{d\vec{y}}{dl} \equiv \vec{R}(\vec{y}), \quad (23)$$

where  $\vec{y} = \{y_i\}$  is the vector of 13 running coupling constants, and  $\vec{R}(\vec{y})$  is a vector function of  $\vec{y}$ . By definition, the fixed points  $\vec{y} = \vec{y}^*$  are given by

$$\vec{R}(\vec{y}^*) = 0. \quad (24)$$

It is obvious that  $\vec{y}^* = 0$  is the trivial Luttinger liquid fixed point. Nontrivial fixed points  $\vec{y}^* \neq 0$  can be found in perturbation as follows.

In perturbation, we are able to find nontrivial fixed points in two different parameter regions of the microscopic Hamiltonian.

(1) For  $0 < J < U/3$ , we have nontrivial fixed points characterized by the following nonvanishing coupling constants,

$$\begin{aligned} y_{3\parallel}^{(1)} &= y_{3\parallel}^{(1)*}, \\ y_{1\perp}^{(2)} &= y_{1\perp}^{(2)*}, \\ x_{3\parallel}^{(1)} &= x_{3\parallel}^{(1)*}, \end{aligned} \quad (25)$$

while other coupling constants are all zero.

(2) For  $J > U/3$ , nontrivial fixed points are given by

$$\begin{aligned} y_{2\parallel}^{(1)} &= y_{2\parallel}^{(1)*}, \\ y_{1\perp}^{(2)} &= y_{1\perp}^{(2)*}, \end{aligned} \quad (26)$$

while other coupling constants equal zero.

These nontrivial fixed points form hypersurfaces in the 13-dimensional parameter space of coupling constants. By examining the RG flow around these hypersurfaces, we find that these fixed points are phase transition points rather than stable fixed points describing stable phases. Then we shall analyze the RG flow near the fixed points using one-loop RG equations to find out what kind of instabilities are favored.

In the vicinity of the fixed points, the RG equations can be expanded to linear order

$$\vec{R}(\vec{y}) = \vec{R}((\vec{y} - \vec{y}^*) + \vec{y}^*) \simeq W(\vec{y} - \vec{y}^*), \quad (27)$$

where the  $W$  matrix is defined as

$$W_{ab} = \left. \frac{\partial R_a}{\partial y_b} \right|_{\vec{y}=\vec{y}^*}. \quad (28)$$

We diagonalize the  $W$  matrix with the left-eigenvectors  $\phi_\alpha$ ,

$$\phi_\alpha^T W = \phi_\alpha^T \lambda_\alpha, \quad (29)$$

where  $\lambda_\alpha$  are corresponding eigenvalues. The scaling fields are defined as

$$v_\alpha = \phi_\alpha^T (\vec{y} - \vec{y}^*). \quad (30)$$

Under renormalization group these scaling fields shows different behaviors,

$$\begin{aligned} \frac{dv_\alpha}{dl} &= \phi_\alpha^T \frac{d}{dl} (\vec{y} - \vec{y}^*) = \phi_\alpha^T W (\vec{y} - \vec{y}^*) = \lambda_\alpha \phi_\alpha^T (\vec{y} - \vec{y}^*) \\ &= \lambda_\alpha v_\alpha, \end{aligned} \quad (31)$$

which becomes relevant, irrelevant and marginal when  $\lambda_\alpha > 0$ ,  $\lambda_\alpha < 0$  and  $\lambda_\alpha = 0$ , respectively.

Notice that  $\{y_{1\perp}^{(1)}, y_{2\parallel}^{(1)}, y_{2\perp}^{(1)}, y_{3\parallel}^{(1)}, y_{3\perp}^{(1)}, y_{4\perp}^{(1)}, y_{1\perp}^{(2)}, y_{3\perp}^{(2)}\}$  and  $\{x_{1\perp}^{(1)}, x_{3\parallel}^{(1)}, x_{3\perp}^{(1)}, x_{3\perp}^{(2)}, y_{\perp}^{(1)}\}$  form two separated sets in Eqs. (22). The  $W$  matrix is block diagonal as follows,

$$W = \begin{pmatrix} W_1 & 0 \\ 0 & W_2 \end{pmatrix}, \quad (32)$$

where  $W_1$  is a  $8 \times 8$  matrix and  $W_2$  is a  $5 \times 5$  matrix.

To illustrate how to carry out the analysis, we firstly consider a simplified case, say, special fixed points when  $J > U/3$ ,

$$y_{1\perp}^{(2)} = y_{1\perp}^{(2)*}, \quad (33)$$

with other coupling constants equal zero. In this case,  $W_2 = 0$ , and  $W_1$  matrix reads

$$W_1 = \begin{pmatrix} 0 & 0 & -y_{1\perp}^{(2)*} & 0 & 0 & 0 & 0 & 0 \\ 0 & 0 & 0 & 0 & 0 & 0 & 0 & 0 \\ -y_{1\perp}^{(2)*} & 0 & 0 & 0 & 0 & 0 & 0 & 0 \\ 0 & 0 & 0 & 0 & 0 & 0 & 0 & 0 \\ 0 & 0 & 0 & 0 & 0 & 0 & 0 & 0 \\ 0 & 0 & 0 & 0 & 0 & 0 & 0 & 0 \\ -\frac{1}{2}y_{1\perp}^{(2)*} & 0 & 0 & 0 & 0 & y_{1\perp}^{(2)*} & 0 & 0 \\ 0 & 0 & 0 & 0 & 0 & 0 & 0 & 0 \end{pmatrix}. \quad (34)$$

For this non-symmetric matrix, we find that there are only two nonzero eigenvalues,  $-y_{1\perp}^{(2)*}$  with corresponding eigenvector  $y_{1\perp}^{(1)} + y_{2\perp}^{(1)}$  and  $y_{1\perp}^{(2)*}$  with eigenvector  $y_{1\perp}^{(1)} - y_{2\perp}^{(1)}$ . According to the microscopic model, the initial value  $g_{1\perp}^{(2)} = J > 0$ . Then we expect  $y_{1\perp}^{(2)*} > 0$  in the perturbation RG. Thus the relevant scaling field is given by the eigenvector corresponding to the eigenvalue  $y_{1\perp}^{(2)*}$ , say,

$$y_{1\perp}^{(1)} - y_{2\perp}^{(1)}. \quad (35)$$

Then we can extract relevant terms from the bosonic Hamiltonian  $H_{int}^B$ . Thus the low energy effective interacting Hamiltonian becomes

$$\begin{aligned} H_{int}^B &= - \left( g_{1\perp}^{(1)} - g_{2\perp}^{(1)} \right) \frac{2}{(2\pi a)^2} \int dx \cos \left( \frac{2}{\sqrt{3}} \tilde{\phi}_{s-1} + \frac{4}{\sqrt{6}} \tilde{\phi}_{s0} \right) \cos \left( 2\tilde{\theta}_{s+1} \right) \\ &\quad - \left( g_{1\perp}^{(1)} - g_{2\perp}^{(1)} \right) \frac{2}{(2\pi a)^2} \int dx \cos \left( 2\tilde{\phi}_{c+1} \right) \cos \left( \frac{2}{\sqrt{3}} \tilde{\phi}_{s-1} + \frac{4}{\sqrt{6}} \tilde{\phi}_{s0} \right). \end{aligned} \quad (36)$$

When  $J > U/3$ , the initial value of  $y_{1\perp}^{(1)} - y_{2\perp}^{(1)} \propto 3J - U$  is positive. This relevant scaling field will flow to strong coupling and lock the corresponding bosonic fields

around the saddle points,

$$\begin{aligned} \left( \frac{1}{\sqrt{3}} \tilde{\phi}_{s-1} + \frac{2}{\sqrt{6}} \tilde{\phi}_{s0}, \tilde{\phi}_{c+1}, \tilde{\theta}_{s+1} \right) &= (0, 0, 0) \\ \text{or } \left( \frac{\pi}{2}, \frac{\pi}{2}, \frac{\pi}{2} \right). \end{aligned} \quad (37)$$



TABLE II. Possible ordered ground states from one-loop RG analysis when  $J > U/3$ .

| Scaling field   | $y_{2\perp}^{(1)} + y_{4\perp}^{(1)}$   | $y_{1\perp}^{(1)} - y_{2\perp}^{(1)}$   |
|-----------------|---|---|
| Instability     | SDW   | TSC   |
| Order parameter | $O_{ph}^{03} + \frac{\sqrt{3}}{2}O_{ph}^{83}$   | $O_{pp}^{23}$   |
| Saddle point    | $\frac{1}{\sqrt{3}}\tilde{\phi}_{s-1} + \frac{2}{\sqrt{6}}\tilde{\phi}_{s0} = 0 \left(\frac{\pi}{2}\right)$<br>$\tilde{\phi}_{c+1} = \frac{\pi}{2} (0)$<br>$\tilde{\phi}_{s+1} = \frac{\pi}{2} (0)$ | $\frac{1}{\sqrt{3}}\tilde{\phi}_{s-1} + \frac{2}{\sqrt{6}}\tilde{\phi}_{s0} = 0 \left(\frac{\pi}{2}\right)$<br>$\tilde{\phi}_{c+1} = 0 \left(\frac{\pi}{2}\right)$<br>$\tilde{\theta}_{s+1} = 0 \left(\frac{\pi}{2}\right)$ |

and

$$W_2 = \begin{pmatrix} 0 & 0 & x_{3\parallel}^{(1)*} & 0 & 0 \\ -\frac{1}{2}x_{3\parallel}^{(1)*} & 0 & 0 & 0 & 0 \\ x_{3\parallel}^{(1)*} & 0 & 0 & 0 & 0 \\ 0 & 0 & 0 & 0 & 0 \\ 0 & 0 & 0 & 0 & 0 \end{pmatrix}. \quad (40b)$$

These matrices have five nonzero eigenvalues totally, three from  $W_1$  and two from  $W_2$ . The three nonzero eigenvalues from  $W_1$  are  $y_{1\perp}^{(2)*}$ ,  $\pm\sqrt{(y_{3\parallel}^{(1)*})^2 + (y_{1\perp}^{(2)*})^2}$ , and the two from  $W_2$  are  $\pm x_{3\parallel}^{(1)*}$ . Since the related initial values are  $g_{3\parallel}^{(1)} = 0$ ,  $g_{1\perp}^{(2)} = J$ , and  $f_{3\parallel}^{(1)} = 0$ . We expect  $y_{1\perp}^{(2)*} > 0$  in perturbation theory. Moreover, considering the one-loop RG flow around the LL fixed point, we can deduce that  $y_{3\parallel}^{(1)*} > 0$  and  $x_{3\parallel}^{(1)*} > 0$ .

Similar analysis can be carried out as in the situation when  $J > U/3$ . The RG trajectory will flow to three strong coupling limits with relevant scaling fields,  $x_{1\perp}^{(1)} + x_{3\perp}^{(1)}$ ,  $y_{1\perp}^{(1)} + y_{3\perp}^{(1)}$ , and  $y_{1\perp}^{(1)} - y_{2\perp}^{(1)}$ . These relevant scaling fields are associated with positive eigenvalues of  $W$  matrix,  $x_{3\parallel}^{(1)*}$ ,  $y_{3\parallel}^{(1)*}$  and  $y_{1\perp}^{(2)*}$  respectively. They give rise to two different SDW states (one with order parameter  $O_{ph}^{43}$  and  $O_{ph}^{63}$  the other with order parameter  $O_{ph}^{13}$ ) and one spin-singlet superconducting (SSC) state (with order parameter  $O_{pp}^{20}$ ). All these possible ordered ground states for  $0 < J < U/3$  and corresponding order parameters are summarized in Table III.

Then we will compare these three instabilities and find out the strongest one, which is determined by the largest eigenvalue of  $W$  matrix. In the spirit of perturbation theory, we still assume that  $\vec{y}^*$  close to the initial value of  $\vec{y}$ . Note that related initial values are  $g_{3\parallel}^{(1)} = f_{3\parallel}^{(1)} = 0$  and  $g_{1\perp}^{(2)} = J$ , we conclude that the SSC state with order parameter  $O_{pp}^{20}$  will dominate among these three possible ground states.

Now we are ready to summarize the one-loop RG analysis and present the phase diagram. One-loop RG equations have been derived using OPE and several possible instabilities against the Luttinger liquid fixed point have

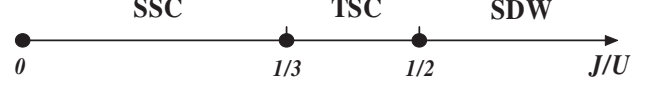


FIG. 5. Phase diagram for the three-band Hubbard model with two degenerate  $E'$  orbitals,  $k_{F+1} = k_{F-1}$ .

been found in weak coupling as summarized in Table II and III. When  $0 < J < U/3$ , the most relevant instability is the spin-singlet SC instability with order parameter  $O_{pp}^{20}$ . When  $U/3 < J < U/2$ , the spin-triplet SC instability with order parameter  $O_{pp}^{23}$  is favored. In the unphysical region  $J > U/2$ , (for  $U = U' + 2J$ ), the spin density wave instability with order parameter  $O_{ph}^{03}$  will dominate. The phase diagram is shown in Fig. 5.

## VII. DISCUSSIONS AND CONCLUSIONS

Now we shall relate our theory to experimental results of  $K_2Cr_3As_3$ . Firstly, we would like to discuss NMR and NQR experiments. The spin-lattice relaxation rate  $1/T_1$  in a NMR experiment measuring the local spin correlation which sums over  $q$  in the momentum space. The dominant contribution comes from  $q \sim 0$  and  $q \sim 2k_F$  components. For a three-band Luttinger liquid governed by the Hamiltonian  $H_0^B$  in Eq. (11), we have the following temperature dependence of  $1/T_1$  (see Appendix C for details),

$$\frac{1}{T_1} \propto A T + B T^{1 - \frac{U}{2\pi v_F}}, \quad (41)$$

where  $U$  is the effective on-site intra-orbital electron interaction. The first linearly temperature dependent term follows Korringa law as in Fermi liquids. The second term follows power law with a non-integer exponent as long as  $U \neq 0$ . When electron Coulomb repulsion governs the system,  $U$  is positive, the dominant contribution at low temperatures will come from the second term. The spin-lattice relaxation rate  $1/T_1$  will exhibit non-integer power law temperature dependence. However,  $U$  may become negative effectively, e.g., when electron-phonon

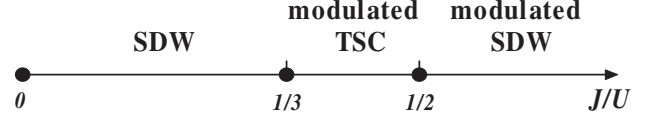
TABLE III. Possible ordered ground states from one-loop RG analysis when  $0 < J < U/3$ .

| Scaling field   | $x_{1\perp}^{(1)} + x_{3\perp}^{(1)}$   | $y_{1\perp}^{(1)} + y_{3\perp}^{(1)}$  | $y_{1\perp}^{(1)} - y_{2\perp}^{(1)}$   |
|-----------------|---|--|---|
| Instability     | SDW   | SDW  | SSC   |
| Order parameter | $O_{ph}^{43}, O_{ph}^{63}$  | $O_{ph}^{13}$  | $O_{pp}^{20}$   |
| Saddle point    | $\frac{1}{2}\tilde{\phi}_{s+1} - \frac{1}{\sqrt{12}}\tilde{\phi}_{s-1} + \frac{2}{\sqrt{6}}\tilde{\phi}_{s0} = 0 \left(\frac{\pi}{2}\right)$<br>$\frac{1}{2}\tilde{\theta}_{c+1} + \frac{3}{\sqrt{12}}\tilde{\theta}_{c-1} = \frac{\pi}{2} (0)$<br>$\frac{1}{2}\tilde{\theta}_{s+1} + \frac{3}{\sqrt{12}}\tilde{\theta}_{s-1} = 0 \left(\frac{\pi}{2}\right)$ | $\frac{1}{\sqrt{3}}\tilde{\phi}_{s-1} + \frac{2}{\sqrt{6}}\tilde{\phi}_{s0} = 0 \left(\frac{\pi}{2}\right)$<br>$\tilde{\theta}_{c+1} = \frac{\pi}{2} (0)$<br>$\tilde{\theta}_{s+1} = 0 \left(\frac{\pi}{2}\right)$ | $\frac{1}{\sqrt{3}}\tilde{\phi}_{s-1} + \frac{2}{\sqrt{6}}\tilde{\phi}_{s0} = 0 \left(\frac{\pi}{2}\right)$<br>$\tilde{\phi}_{c+1} = \frac{\pi}{2} (0)$<br>$\tilde{\theta}_{s+1} = \frac{\pi}{2} (0)$ |

interaction dominates over Coulomb repulsion. In this case,  $1/T_1$  will become linearly temperature dependent at low temperatures as in Fermi liquids. It is consistent with the well-known single-band result that SDW will become irrelevant when  $U < 0$ . In the NQR experiment on  $K_2Cr_3As_3$ ,  $1/T_1$  exhibit non-integer power law temperature dependence and gives rise to  $1 - \frac{U}{2\pi v_F} \sim 0.75$ . However, the NQR experiment on  $Rb_2Cr_3As_3$  shows linear temperature dependence at high temperature while critical spin fluctuations appear near to the SC transition temperature  $T_c$ . These diversified  $1/T_1$  behaviors in  $K_2Cr_3As_3$  and  $Rb_2Cr_3As_3$  imply different effective electron in the two systems. The Rb compound has large unit cell volume than K compound, resulting in a smaller electron repulsion, which is consistent with larger exponent,  $1 - \frac{U}{2\pi v_F} \sim 1$  in  $1/T_1$  in  $Rb_2Cr_3As_3$ .

We next discuss two possible SC ground states in physical parameter regions  $0 < J < U/3$  and  $U/3 < J < U/2$ . (1) At  $0 < J < U/3$ , the order parameter  $O_{pp}^{20}$  indicates that the SC pairing is spin-singlet and orbital antisymmetric, and the pairing electrons come from the two degenerate  $E'$  bands. (2) While for  $U/3 < J < U/2$ , the order parameter  $O_{pp}^{23}$  gives rise to spin-triplet ( $|\uparrow\downarrow\rangle + |\downarrow\uparrow\rangle$ ) and orbital antisymmetric SC pairing, and the pairing electrons come from  $E'$  bands too. This kind of even-parity, spin-triplet and orbital antisymmetric SC pairing was firstly proposed by Dai *et al.* in the context of iron-pnictide<sup>26</sup>. Note that the degeneracy of two  $E'$  bands plays a crucial role in the formation of SC ground states.

The role of the two degenerate  $E'$  bands can be also seen from the effective Hamiltonian  $H_{int}^B$  and order parameters for different ground states. To do this, we consider the situation when the two-fold degeneracy is slightly lifted, for instance, by inter-chain coupling. In this case, we have  $k_{F+1} \neq k_{F-1}$ . Introducing  $\Delta k_F = k_{F+1} - k_{F-1}$ , we can generalize the bosonic interacting Hamiltonian in Eq. (13) to the expression in Eq. (D1) in Appendix D, where an additional phase factor  $2\Delta k_F x$  appears in  $g_{2\parallel}^{(1)}$ ,  $g_{2\perp}^{(1)}$  and  $g_{1\perp}^{(2)}$  terms. Thus these terms will be suppressed by this phase factor in the integrand. Consequently, both the spin-triplet SC order parameter  $O_{pp}^{20}$  (for  $U/3 < J < U/2$ ) and the spin-singlet SC order parameter  $O_{pp}^{23}$  (for  $0 < J < U/3$ ) will be suppressed and be modulated by the phase factor  $2\Delta k_F x$ , indicating a

FIG. 6. Phase diagram for the three-band Hubbard model with lifted degeneracy in  $E'$  orbitals,  $k_{F+1} \neq k_{F-1}$ .

possible FFLO state when  $\Delta k_F \neq 0$ <sup>27,28</sup>. This is because that both  $O_{pp}^{20}$  and  $O_{pp}^{23}$  arise from inter-orbital pairing, namely, pairing between  $\pm k_{F+1}$  and  $\mp k_{F-1}$ .

Then we shall investigate how the lifted degeneracy will affect the SDW ground states characterized by order parameters,  $O_{ph}^{03} + \frac{\sqrt{3}}{2}O_{ph}^{83}$ ,  $O_{ph}^{43}(O_{ph}^{63})$ , and  $O_{ph}^{13}$  respectively. The expression for  $O_{ph}^{43}(O_{ph}^{63})$  and  $O_{ph}^{13}$  will not change as we turn on  $\Delta k_F$ . Since SDW instabilities in these states come from the scattering from  $\pm k_{F+}$  to  $\mp k_{F-}$ . However, the order parameter  $O_{ph}^{03} + \frac{\sqrt{3}}{2}O_{ph}^{83}$  arising from intra-orbital scattering, say, from  $\pm k_{F+1}$  to  $\pm k_{F-1}$ , will be suppressed and be modulated by the phase factor  $2\Delta k_F x$  too.

Thus, we expect that (1) for  $0 < J < U/3$ , the SDW states will win out since the SSC state is suppressed; (2) for  $U/3 < J < U/2$ , the TSC state will survive and be modulated by a phase factor  $2\Delta k_F x$ , since the possible competing SDW order ( $O_{ph}^{03} + \frac{\sqrt{3}}{2}O_{ph}^{83}$ ) will be suppressed too; (3) for the unphysical region  $J > U/2$ , the SDW state will be modulated by a phase factor  $2\Delta k_F x$ . The new phase diagram is illustrated in Fig. 6.

Finally, we would like to figure out that these ordered states will not survive in a single chain due to strong quantum fluctuations, as stated by Mermin-Wagner-Hohenberg theorem<sup>29,30</sup>. However, these instabilities will be enhanced at low temperatures. So that small inter-chain couplings will stabilize these ordered states. Moreover, the inter-chain couplings will also determine the spatial pairing symmetry for SC states. Work along this line is under progress.

In summary, we have studied a three-band Hubbard model at incommensurate filling with intra-orbital electron repulsion  $U$ , inter-orbital electron repulsion  $U'$ , and

Hund's coupling  $J > 0$ , which satisfy that  $U = U' + 2J$ . With the help of bosonization and RG, we find that the Luttinger fixed point gives rise to the experimental observed normal state at high temperature. The ground state instability depends on the ratio  $J/U$  and the degeneracy of  $E'$  bands. When the two  $E'$  bands are degenerate, for  $0 < J < U/2$ , the ground state is a spin-singlet SC state; for  $U/3 < J < U/2$ , a spin-singlet SC state is favored; a SDW state can be achieved in the unphysical parameter region  $J > U/2$ . However, when the two-fold degeneracy of  $E'$  bands is lifted, the phase diagram will change. In the physically relevant regions, a SDW state may dominate instead of the spin-singlet SC state when  $0 < J < U/3$ , the spin-triplet SC state is still favored when  $U/3 < J < U/2$ ; but the SC order parameter will be modulated by a spatially varying phase factor  $2\Delta k_F x$ . Our theoretical results support the existence of a spin-triplet SC state in  $K_2Cr_3As_3$ .

### VIII. ACKNOWLEDGEMENT

We would like to thank Guang-Han Cao, Chao Cao, Jian-Hui Dai, Xiao-Yong Feng for helpful discussions, and thank Jun-ichi Okamoto and A. J. Millis for the communications on the two-band situation. This work is partially supported by National Basic Research Program of China (No.2014CB921201/2014CB921203), NSFC (No.11374256/11274269), and the Fundamental Research Funds for the Central Universities in China.

#### Appendix A: Derivation of tree-level RG equations

The tree-level RG equations are given by the scaling dimension  $\Delta_k$  for each coupling constant  $g_k$ . Since  $\Delta_k$  is determined by Luttinger parameters  $K_{\mu\nu}$ , one finds that

$$\frac{dg_{1\perp}^{(1)}}{dl} = \left[ 2 - \left( \frac{1}{3}K_{s-1} + \frac{2}{3}K_{s0} + K_{s+1}^{-1} \right) \right] g_{1\perp}^{(1)}, \quad (\text{A1a})$$

$$\frac{dg_{2\parallel}^{(1)}}{dl} = [2 - (K_{c+1} + K_{s+1})] g_{2\parallel}^{(1)}, \quad (\text{A1b})$$

$$\frac{dg_{2\perp}^{(1)}}{dl} = \left[ 2 - \left( K_{c+1} + \frac{1}{3}K_{s-1} + \frac{2}{3}K_{s0} \right) \right] g_{2\perp}^{(1)}, \quad (\text{A1c})$$

$$\frac{dg_{3\parallel}^{(1)}}{dl} = [2 - (K_{c+1}^{-1} + K_{s+1}^{-1})] g_{3\parallel}^{(1)}, \quad (\text{A1d})$$

$$\frac{dg_{3\perp}^{(1)}}{dl} = \left[ 2 - \left( K_{c+1}^{-1} + \frac{1}{3}K_{s-1} + \frac{2}{3}K_{s0} \right) \right] g_{3\perp}^{(1)}, \quad (\text{A1e})$$

$$\frac{dg_{4\perp}^{(1)}}{dl} = \left[ 2 - \left( K_{c+1} + \frac{1}{3}K_{s-1} + \frac{2}{3}K_{s0} \right) \right] g_{4\perp}^{(1)}, \quad (\text{A1f})$$

$$\frac{dg_{1\perp}^{(2)}}{dl} = [2 - (K_{c+1} + K_{s+1}^{-1})] g_{1\perp}^{(2)}, \quad (\text{A1g})$$

$$\frac{dg_{3\perp}^{(2)}}{dl} = [2 - (K_{c+1}^{-1} + K_{s+1})] g_{3\perp}^{(2)}, \quad (\text{A1h})$$

$$\frac{df_{1\perp}^{(1)}}{dl} = \left[ 2 - \left( \frac{1}{4}K_{s+1} + \frac{1}{12}K_{s-1} + \frac{2}{3}K_{s0} + \frac{1}{4}K_{s+1}^{-1} + \frac{3}{4}K_{s-1}^{-1} \right) \right] f_{1\perp}^{(1)}, \quad (\text{A1i})$$

$$\frac{df_{3\parallel}^{(1)}}{dl} = \left[ 2 - \left( \frac{1}{4}K_{c+1}^{-1} + \frac{3}{4}K_{c-1}^{-1} + \frac{1}{4}K_{s+1}^{-1} + \frac{3}{4}K_{s-1}^{-1} \right) \right] \times f_{3\parallel}^{(1)}, \quad (\text{A1j})$$

$$\frac{df_{3\perp}^{(1)}}{dl} = \left[ 2 - \left( \frac{1}{4}K_{c+1}^{-1} + \frac{3}{4}K_{c-1}^{-1} + \frac{1}{4}K_{s+1} + \frac{1}{12}K_{s-1} + \frac{2}{3}K_{s0} \right) \right] f_{3\perp}^{(1)}, \quad (\text{A1k})$$

$$\frac{df_{3\perp}^{(2)}}{dl} = \left[ 2 - \left( \frac{1}{4}K_{c+1}^{-1} + \frac{3}{4}K_{c-1}^{-1} + \frac{1}{4}K_{s+1} + \frac{3}{4}K_{s-1} \right) \right] \times f_{3\perp}^{(2)}, \quad (\text{A1l})$$

$$\frac{dg_{\perp}^{(1)}}{dl} = \left[ 2 - \left( \frac{4}{3}K_{s-1} + \frac{2}{3}K_{s0} \right) \right] g_{\perp}^{(1)}. \quad (\text{A1m})$$

To simplify, we introduce the renormalized coupling constants  $x_i$  and  $y_i$  as defined in Eq. (20). In weak coupling, we can expand Luttinger liquid parameters  $K_{\mu\nu}$  to leading order of  $x_i$  and  $y_i$ 's,

$$K_{\mu\nu} = 1 - y_{\mu\nu}, \quad (\text{A2})$$

where the redefined Luttinger liquid parameters  $y_{\mu\nu}$  are linear combinations of  $y_i$ 's,

$$y_{c\pm 1} = \frac{1}{2} \left[ \left( y_{4\perp}^{(2)} \right) - \left( y_{2\parallel}^{(2)} + y_{2\perp}^{(2)} \right) \right], \quad (\text{A3a})$$

$$y_{c0} = \frac{1}{2} \left[ \left( y_{4\perp}^{(2)} \right) + 2 \left( y_{2\parallel}^{(2)} + y_{2\perp}^{(2)} \right) \right], \quad (\text{A3b})$$

$$y_{s\pm 1} = \frac{1}{2} \left[ \left( -y_{4\perp}^{(2)} \right) - \left( y_{2\parallel}^{(2)} - y_{2\perp}^{(2)} \right) \right], \quad (\text{A3c})$$

$$y_{s0} = \frac{1}{2} \left[ \left( -y_{4\perp}^{(2)} \right) + 2 \left( y_{2\parallel}^{(2)} - y_{2\perp}^{(2)} \right) \right]. \quad (\text{A3d})$$

Then the tree-level RG equations Eqs. (A1) can be written in terms of  $x_i$  and  $y_i$ 's as in Eqs. (21).

## Appendix B: Derivation of one-loop RG equations

The full structure constants  $C_{ij}^k$  in OPE in Eq. (19) can be obtained by the fusion of arbitrary two terms in the interaction  $H_{int}^B$ . This processes will generate new terms, which are absent in the original microscopic Hamiltonian, until all terms form a closed algebra. Thus we should retain the related terms with zero initial values of coupling constants. The one-loop RG equations from OPE read,

$$\frac{dy_{1\perp}^{(1)}}{dl} = \left( y_{2\parallel}^{(2)} - y_{2\perp}^{(2)} \right) y_{1\perp}^{(1)} - y_{2\perp}^{(1)} y_{1\perp}^{(2)} + y_{3\parallel}^{(1)} y_{3\perp}^{(1)}, \quad (\text{B1a})$$

$$\frac{dy_{2\parallel}^{(1)}}{dl} = -y_{2\parallel}^{(2)} y_{2\parallel}^{(1)} - y_{2\perp}^{(1)} y_{4\perp}^{(1)}, \quad (\text{B1b})$$

$$\frac{dy_{2\perp}^{(1)}}{dl} = -y_{2\perp}^{(2)} y_{2\perp}^{(1)} - y_{1\perp}^{(1)} y_{1\perp}^{(2)} - y_{2\parallel}^{(1)} y_{4\perp}^{(1)}, \quad (\text{B1c})$$

$$\frac{dy_{3\parallel}^{(1)}}{dl} = y_{2\parallel}^{(2)} y_{3\parallel}^{(1)} + y_{1\perp}^{(1)} y_{3\perp}^{(1)}, \quad (\text{B1d})$$

$$\frac{dy_{3\perp}^{(1)}}{dl} = \left( -y_{4\perp}^{(2)} + y_{2\parallel}^{(2)} \right) y_{3\perp}^{(1)} + y_{1\perp}^{(1)} y_{3\parallel}^{(1)} - y_{4\perp}^{(1)} y_{3\perp}^{(2)}, \quad (\text{B1e})$$

$$\frac{dy_{4\perp}^{(1)}}{dl} = -y_{2\perp}^{(2)} y_{4\perp}^{(1)} - y_{2\parallel}^{(1)} y_{2\perp}^{(1)} - y_{3\perp}^{(1)} y_{3\perp}^{(2)}, \quad (\text{B1f})$$

$$\frac{dy_{1\perp}^{(2)}}{dl} = \left( y_{4\perp}^{(2)} - y_{2\perp}^{(2)} \right) y_{1\perp}^{(2)} - y_{1\perp}^{(1)} y_{2\perp}^{(1)}, \quad (\text{B1g})$$

$$\frac{dy_{3\perp}^{(2)}}{dl} = \left( -y_{4\perp}^{(2)} + y_{2\parallel}^{(2)} \right) y_{3\perp}^{(2)} - y_{3\perp}^{(1)} y_{4\perp}^{(1)}, \quad (\text{B1h})$$

$$\frac{dx_{1\perp}^{(1)}}{dl} = \left( y_{2\parallel}^{(2)} - y_{2\perp}^{(2)} \right) x_{1\perp}^{(1)} + x_{3\parallel}^{(1)} x_{3\perp}^{(1)}, \quad (\text{B1i})$$

$$\frac{dx_{3\parallel}^{(1)}}{dl} = y_{2\parallel}^{(2)} x_{3\parallel}^{(1)} + x_{1\perp}^{(1)} x_{3\perp}^{(1)}, \quad (\text{B1j})$$

$$\frac{dx_{3\perp}^{(1)}}{dl} = \left( -y_{4\perp}^{(2)} + y_{2\parallel}^{(2)} \right) x_{3\perp}^{(1)} + x_{1\perp}^{(1)} x_{3\parallel}^{(1)}, \quad (\text{B1k})$$

$$\frac{dx_{3\perp}^{(2)}}{dl} = \left( -y_{4\perp}^{(2)} + y_{2\perp}^{(2)} \right) x_{3\perp}^{(2)}, \quad (\text{B1l})$$

$$\frac{dy_{\perp}^{(1)}}{dl} = -y_{4\perp}^{(2)} y_{\perp}^{(1)}. \quad (\text{B1m})$$

As mentioned in Section VI.1 in the main text, we should restore the spin rotational symmetry by imposing the following constraints on coupling constants,

$$g_{1\parallel}^{(1)} - g_{2\parallel}^{(2)} = g_{1\perp}^{(1)} - g_{2\perp}^{(2)}, \quad (\text{B2a})$$

$$g_{2\parallel}^{(1)} - g_{1\parallel}^{(2)} = g_{2\perp}^{(1)} - g_{1\perp}^{(2)}, \quad (\text{B2b})$$

$$g_{3\parallel}^{(1)} - g_{3\parallel}^{(2)} = g_{3\perp}^{(1)} - g_{3\perp}^{(2)}, \quad (\text{B2c})$$

$$g_{4\parallel}^{(1)} - g_{4\parallel}^{(2)} = g_{4\perp}^{(1)} - g_{4\perp}^{(2)}, \quad (\text{B2d})$$

$$f_{1\parallel}^{(1)} - f_{2\parallel}^{(2)} = f_{1\perp}^{(1)} - f_{2\perp}^{(2)}, \quad (\text{B2e})$$

$$f_{2\parallel}^{(1)} - f_{1\parallel}^{(2)} = f_{2\perp}^{(1)} - f_{1\perp}^{(2)}, \quad (\text{B2f})$$

$$f_{3\parallel}^{(1)} - f_{3\parallel}^{(2)} = f_{3\perp}^{(1)} - f_{3\perp}^{(2)}, \quad (\text{B2g})$$

$$g_{\parallel}^{(1)} - g_{\parallel}^{(2)} = g_{\perp}^{(1)} - g_{\perp}^{(2)}. \quad (\text{B2h})$$

which will simplify our analysis. In addition to these spin  $SU(2)$  constraints, we also have

$$g_{4\perp}^{(2)} = g_{\perp}^{(2)}, \quad (\text{B3a})$$

$$g_{2\parallel}^{(2)} = f_{2\parallel}^{(2)}, \quad (\text{B3b})$$

$$g_{2\perp}^{(2)} = f_{2\perp}^{(2)}, \quad (\text{B3c})$$

from the microscopic Hamiltonian. By these relations, we have

$$\frac{dy_{1\perp}^{(1)}}{dl} = - \left( y_{1\perp}^{(1)} \right)^2 - y_{2\perp}^{(1)} y_{1\perp}^{(2)} + y_{3\parallel}^{(1)} y_{3\perp}^{(1)}, \quad (\text{B4a})$$

$$\frac{dy_{2\parallel}^{(1)}}{dl} = - \frac{1}{2} \left( y_{2\parallel}^{(2)} + y_{2\perp}^{(2)} - y_{1\perp}^{(1)} \right) y_{2\parallel}^{(1)} - y_{2\perp}^{(1)} y_{4\perp}^{(1)}, \quad (\text{B4b})$$

$$\begin{aligned} \frac{dy_{2\perp}^{(1)}}{dl} = & - \frac{1}{2} \left( y_{2\parallel}^{(2)} + y_{2\perp}^{(2)} + y_{1\perp}^{(1)} \right) y_{2\perp}^{(1)} - y_{1\perp}^{(1)} y_{1\perp}^{(2)} \\ & - y_{2\parallel}^{(1)} y_{4\perp}^{(1)}, \end{aligned} \quad (\text{B4c})$$

$$\frac{dy_{3\parallel}^{(1)}}{dl} = \frac{1}{2} \left( y_{2\parallel}^{(2)} + y_{2\perp}^{(2)} - y_{1\perp}^{(1)} \right) y_{3\parallel}^{(1)} + y_{1\perp}^{(1)} y_{3\perp}^{(1)}, \quad (\text{B4d})$$

$$\begin{aligned} \frac{dy_{3\perp}^{(1)}}{dl} = & \left( -y_{4\perp}^{(1)} + \frac{1}{2} \left( y_{2\parallel}^{(2)} + y_{2\perp}^{(2)} - y_{1\perp}^{(1)} \right) \right) y_{3\perp}^{(1)} \\ & + y_{1\perp}^{(1)} y_{3\parallel}^{(1)} - y_{4\perp}^{(1)} y_{3\perp}^{(2)}, \end{aligned} \quad (\text{B4e})$$

$$\begin{aligned} \frac{dy_{4\perp}^{(1)}}{dl} = & - \frac{1}{2} \left( y_{2\parallel}^{(2)} + y_{2\perp}^{(2)} - y_{1\perp}^{(1)} \right) y_{4\perp}^{(1)} - y_{2\parallel}^{(1)} y_{2\perp}^{(1)} \\ & - y_{3\perp}^{(1)} y_{3\perp}^{(2)}, \end{aligned} \quad (\text{B4f})$$

$$\begin{aligned} \frac{dy_{1\perp}^{(2)}}{dl} = & \left( y_{4\perp}^{(1)} - \frac{1}{2} \left( y_{2\parallel}^{(2)} + y_{2\perp}^{(2)} + y_{1\perp}^{(1)} \right) \right) y_{1\perp}^{(2)} \\ & - y_{1\perp}^{(1)} y_{2\perp}^{(1)}, \end{aligned} \quad (\text{B4g})$$

$$\begin{aligned} \frac{dy_{3\perp}^{(2)}}{dl} &= \left( -y_{4\perp}^{(1)} + \frac{1}{2} \left( y_{2\parallel}^{(2)} + y_{2\perp}^{(2)} + y_{1\perp}^{(1)} \right) \right) y_{3\perp}^{(2)} \\ &\quad - y_{3\perp}^{(1)} y_{4\perp}^{(1)}, \end{aligned} \quad (\text{B4h})$$

$$\frac{dx_{1\perp}^{(1)}}{dl} = - \left( x_{1\perp}^{(1)} \right)^2 + x_{3\parallel}^{(1)} x_{3\perp}^{(1)}, \quad (\text{B4i})$$

$$\frac{dx_{3\parallel}^{(1)}}{dl} = \frac{1}{2} \left( x_{2\parallel}^{(2)} + x_{2\perp}^{(2)} - x_{1\perp}^{(1)} \right) x_{3\parallel}^{(1)} + x_{1\perp}^{(1)} x_{3\perp}^{(1)}, \quad (\text{B4j})$$

$$\begin{aligned} \frac{dx_{3\perp}^{(1)}}{dl} &= \left( -y_{\perp}^{(1)} + \frac{1}{2} \left( x_{2\parallel}^{(2)} + x_{2\perp}^{(2)} - x_{1\perp}^{(1)} \right) \right) x_{3\perp}^{(1)} \\ &\quad + x_{1\perp}^{(1)} x_{3\parallel}^{(1)}, \end{aligned} \quad (\text{B4k})$$

$$\frac{dx_{3\perp}^{(2)}}{dl} = \left( -y_{\perp}^{(1)} + \frac{1}{2} \left( x_{2\parallel}^{(2)} + x_{2\perp}^{(2)} + x_{1\perp}^{(1)} \right) \right) x_{3\perp}^{(2)}, \quad (\text{B4l})$$

$$\frac{dy_{\perp}^{(1)}}{dl} = - \left( y_{\perp}^{(1)} \right)^2. \quad (\text{B4m})$$

Note that the variables  $y_{2\parallel}^{(2)} + y_{2\perp}^{(2)}$  and  $x_{2\parallel}^{(2)} + x_{2\perp}^{(2)}$  do not flow as they do not appear in  $H_{int}^B$ . In perturbation, we can drop these small variables to obtain closed one-loop RG equations. By keeping all the relevant terms, we have Eqs. (22).

### Appendix C: Spin-lattice relaxation rate for a three-band Tomonaga-Luttinger liquid

The spin-lattice relaxation rate  $1/T_1$  in a NMR experiment detects the local spin correlation function

$$\frac{1}{T_1} = A_f^2 T \sum_q \frac{\text{Im} \chi(q, \omega)}{\omega}, \quad (\text{C1})$$

where  $A_f$  is the hyperfine coupling constant. The spin correlation function in a multi-band system is defined as

$$\chi^{\alpha\beta}(x, \tau) = \sum_m \langle S_m^\alpha(x, \tau) S_m^\beta(0, 0) \rangle \quad (\text{C2})$$

where  $S_m^\alpha = \frac{1}{2} \sum_{ss'} c_{ms}^\dagger \sigma_{ss'}^\alpha c_{ms'}$  is the spin operator in the  $m$ -th band and  $\alpha, \beta = x, y, z$ .

For a system where spin rotational symmetry is respected,  $\chi^{\alpha\beta} = \chi \delta_{\alpha\beta}$ . We find that the dominant contribution to  $\chi$  come from  $q \sim 0$  and  $q \sim 2k_F$  components.

Suming over all the bands, we have the following form of the temperature dependent spin-lattice relaxation rate,

$$\begin{aligned} \frac{1}{T_1} &\propto A_1 T \\ &\quad + A_2 T^{\frac{1}{2}} \left[ (K_{c+1} + \frac{1}{3} K_{c-1} + \frac{2}{3} K_{c0}) + (K_{s+1} + \frac{1}{3} K_{s-1} + \frac{2}{3} K_{s0}) \right]^{-1} \\ &\quad + A_3 T^{\frac{1}{2}} \left[ (\frac{4}{3} K_{c-1} + \frac{2}{3} K_{c0}) + (\frac{4}{3} K_{s-1} + \frac{2}{3} K_{s0}) \right]^{-1}. \end{aligned} \quad (\text{C3})$$

The first linearly temperature dependent term follows Korringa law as in Fermi liquids. The second term comes from the two degenerate bands  $m = \pm 1$  and both have the same exponent. The third term comes from the non-degenerate band  $m = 0$ . In the non-interacting limit,  $K_{\mu\nu} = 1$ , thus all the three terms become linearly temperature dependent as in Fermi liquids.

With the help of spin rotational symmetry, we can further simplify the expression in Eq. (C3). Considering the spin correlation function  $\chi^{\alpha\beta} = \chi \delta_{\alpha\beta}$  in the LL fixed point, the spin  $SU(2)$  symmetry will imposes the following constraints to Luttinger parameters,

$$K_{sm} = 1. \quad (\text{C4})$$

Meanwhile, we have  $K_{c+1} = K_{c-1}$  in our model. In weak coupling, we can expand Luttinger parameters as  $K_{\mu\nu} = 1 - y_{\mu\nu}$ . Then the spin-lattice relaxation rate can be simplified as

$$\frac{1}{T_1} \propto A T + B T^{1 - \frac{y_{4\perp}^{(2)}}{2}}, \quad (\text{C5})$$

where the coupling constant  $y_{4\perp}^{(2)}$  is chosen as its initial value  $y_{4\perp}^{(2)} = U/\pi v_F$ . When the short ranged Coulomb repulsion govern the system,  $U$  is positive, the dominant contribution will come from the second term at low temperatures. The spin-lattice relaxation rate  $1/T_1$  will exhibit non-integer power law temperature dependence. However,  $U$  may become negative effectively, e.g., when electron-phonon interaction dominates. In this case,  $1/T_1$  will become linearly temperature dependent at low temperatures as in Fermi liquids. It is consistent with the common sense that SDW terms will become irrelevant when  $U < 0$ .

### Appendix D: Interacting Hamiltonian $H_{int}^B$ for $k_{F+1} \neq k_{F-1}$

When the degeneracy of the two  $E'$  bands is lifted,  $k_{F+1} \neq k_{F-1}$ . From Eq. (8), we find that the terms containing phase  $\tilde{\phi}_{c+1} \propto \phi_{c+1} - \phi_{c-1}$  should change with a phase factor  $\Delta k_F x$ , resulting in the interacting Hamiltonian  $H_{int}^B$  for  $k_{F+1} \neq k_{F-1}$  as follows,



$$\begin{aligned}
H_{int}^B = & -g_{1\perp}^{(1)} \frac{4}{(2\pi a)^2} \int dx \cos\left(\frac{2}{\sqrt{3}}\tilde{\phi}_{s-1} + \frac{4}{\sqrt{6}}\tilde{\phi}_{s0}\right) \cos\left(2\tilde{\theta}_{s+1}\right) \\
& + g_{2\parallel}^{(1)} \frac{4}{(2\pi a)^2} \int dx \cos\left(2\Delta k_F x + 2\tilde{\phi}_{c+1}\right) \cos\left(2\tilde{\phi}_{s+1}\right) \\
& + g_{2\perp}^{(1)} \frac{4}{(2\pi a)^2} \int dx \cos\left(2\Delta k_F x + 2\tilde{\phi}_{c+1}\right) \cos\left(\frac{2}{\sqrt{3}}\tilde{\phi}_{s-1} + \frac{4}{\sqrt{6}}\tilde{\phi}_{s0}\right) \\
& + g_{3\parallel}^{(1)} \frac{4}{(2\pi a)^2} \int dx \cos\left(2\tilde{\theta}_{c+1}\right) \cos\left(2\tilde{\theta}_{s+1}\right) \\
& + g_{3\perp}^{(1)} \frac{4}{(2\pi a)^2} \int dx \cos\left(2\tilde{\theta}_{c+1}\right) \cos\left(\frac{2}{\sqrt{3}}\tilde{\phi}_{s-1} + \frac{4}{\sqrt{6}}\tilde{\phi}_{s0}\right) \\
& + g_{4\perp}^{(1)} \frac{4}{(2\pi a)^2} \int dx \cos\left(2\tilde{\phi}_{s+1}\right) \cos\left(\frac{2}{\sqrt{3}}\tilde{\phi}_{s-1} + \frac{4}{\sqrt{6}}\tilde{\phi}_{s0}\right) \\
& - g_{1\perp}^{(2)} \frac{4}{(2\pi a)^2} \int dx \cos\left(2\Delta k_F x + 2\tilde{\phi}_{c+1}\right) \cos\left(2\tilde{\theta}_{s+1}\right) \\
& + g_{3\perp}^{(2)} \frac{4}{(2\pi a)^2} \int dx \cos\left(2\tilde{\theta}_{c+1}\right) \cos\left(2\tilde{\phi}_{s+1}\right) \\
& - f_{1\perp}^{(1)} \frac{8}{(2\pi a)^2} \int dx \left[ \cos\tilde{\phi}_{s+1} \cos\left(-\frac{1}{\sqrt{3}}\tilde{\phi}_{s-1} + \frac{4}{\sqrt{6}}\tilde{\phi}_{s0}\right) \cos\tilde{\theta}_{s+1} \cos\sqrt{3}\tilde{\theta}_{s-1} + (\cos \rightarrow \sin) \right] \\
& + f_{3\parallel}^{(1)} \frac{8}{(2\pi a)^2} \int dx \left[ \cos\tilde{\theta}_{c+1} \cos\sqrt{3}\tilde{\theta}_{c-1} \cos\tilde{\theta}_{s+1} \cos\sqrt{3}\tilde{\theta}_{s-1} + (\cos \rightarrow \sin) \right] \\
& + f_{3\perp}^{(1)} \frac{8}{(2\pi a)^2} \int dx \left[ \cos\tilde{\theta}_{c+1} \cos\sqrt{3}\tilde{\theta}_{c-1} \cos\tilde{\phi}_{s+1} \cos\left(-\frac{1}{\sqrt{3}}\tilde{\phi}_{s-1} + \frac{4}{\sqrt{6}}\tilde{\phi}_{s0}\right) + (\cos \rightarrow \sin) \right] \\
& + f_{3\perp}^{(2)} \frac{8}{(2\pi a)^2} \int dx \left[ \cos\tilde{\theta}_{c+1} \cos\sqrt{3}\tilde{\theta}_{c-1} \cos\tilde{\phi}_{s+1} \cos\sqrt{3}\tilde{\phi}_{s-1} + (\cos \rightarrow \sin) \right] \\
& + g_{\perp}^{(1)} \frac{2}{(2\pi a)^2} \int dx \cos\left(-\frac{4}{\sqrt{3}}\tilde{\phi}_{s-1} + \frac{4}{\sqrt{6}}\tilde{\phi}_{s0}\right), \tag{D1}
\end{aligned}$$

where  $\Delta k_F = k_{F+1} - k_{F-1}$ .

- 
- <sup>1</sup> Jin-Ke Bao, Ji-Yong Liu, Cong-Wei Ma, Zhi-Hao Meng, Zhang-Tu Tang, Yun-Lei Sun, Hui-Fei Zhai, Hao Jiang, Hua Bai, Chun-Mu Feng, Zhu-An Xu, Guang-Han Cao, *Phys. Rev. X* 5, 011013 (2015).
  - <sup>2</sup> Zhang-Tu Tang, Jin-Ke Bao, Yi Liu, Yun-Lei Sun, Abduweli Ablimit, Hui-Fei Zhai, Hao Jiang, Chun-Mu Feng, Zhu-An Xu, Guang-Han Cao, *Phys. Rev. B* 91, 020506(R) (2015).
  - <sup>3</sup> Zhang-Tu Tang, Jin-Ke Bao, Zhen Wang, Hua Bai, Hao Jiang, Yi Liu, Hui-Fei Zhai, Chun-Mu Feng, Zhu-An Xu, Guang-Han Cao, *Science China Materials*, 58(1), 16-20 (2015).
  - <sup>4</sup> Guang-Han Cao *et al.*, unpublished.
  - <sup>5</sup> H. Z. Zhi, T. Imai, F. L. Ning, Jin-Ke Bao, Guang-Han Cao, *Phys. Rev. Lett.* 114, 147004 (2015).
  - <sup>6</sup> J. Yang, Z. T. Tang, G. H. Cao, and Guo-qing Zheng, *Phys. Rev. Lett.* 115, 227001 (2015).
  - <sup>7</sup> Tai Kong, Sergey L. Bud'ko, Paul C. Canfield, *Phys. Rev. B* 91, 020507(R) (2015).
  - <sup>8</sup> F. F. Balakirev, T. Kong, M. Jaime, R. D. McDonald, C. H. Mielke, A. Gurevich, P. C. Canfield, and S. L. Bud'ko, *Phys. Rev. B* 91, 220505(R) (2015).
  - <sup>9</sup> Huakun Zuo, Jin-Ke Bao, Yi Liu, Jinhua Wang, Zhao Jin, Zhengcai Xia, Liang Li, Zhuan Xu, Zengwei Zhu, Guang-Han Cao, arXiv:1511.06169 (2015).
  - <sup>10</sup> D. T. Adroja, A. Bhattacharyya, M. Telling, Yu. Feng, M. Smidman, B. Pan, J. Zhao, A. D. Hillier, F. L. Pratt, and A. M. Strydom, *Phys. Rev. B* 92, 134505 (2012).
  - <sup>11</sup> G. M. Pang, M. Smidman, W. B. Jiang, J. K. Bao, Z. F. Weng, Y. F. Wang, L. Jiao, J. L. Zhang, G. H. Cao, H. Q. Yuan, *Phys. Rev. B* 91, 220502(R) (2015).
  - <sup>12</sup> Yi Liu, Jin-Ke Bao, Hao-Kun Zuo, Abduweli Ablimit, Zhang-Tu Tang, Chun-Mu Feng, Zeng-Wei Zhu, Guang-Han Cao, *Science China Physics, Mechanics and Astronomy*, 59(5), 1-5 (2016).
  - <sup>13</sup> Hao Jiang, Guanghan Cao, Chao Cao, *Sci. Rep.* 5, 16054 (2015).

- <sup>14</sup> X. X. Wu, C. C. Le, J. Yuan, H. Fan, and J. P. Hu, *Chin. Phys. Lett.* 32, 057401 (2015).
- <sup>15</sup> Yi Zhou, Chao Cao, Fu-Chun Zhang, arXiv:1502.03928 preprint.
- <sup>16</sup> Xianxin Wu, Fan Yang, Congcong Le, Jing Yuan, Heng Fan, Jiangping Hu, *Phys. Rev. B* 92, 104511 (2015).
- <sup>17</sup> Li-Da Zhang, Xianxin Wu, Heng Fan, Fan Yang, Jiangping Hu, arXiv:1512.00147 (2015).
- <sup>18</sup> Xianxin Wu, Fan Yang, Shengshan Qin, Heng Fan, Jiangping Hu, arXiv:1507.07451 (2015).
- <sup>19</sup> Hanting Zhong, Xiao-Yong Feng, Hua Chen, and Jianhui Dai, *Phys. Rev. Lett.* 115, 227001 (2015).
- <sup>20</sup> P. Chudzinski, M. Gabay, and T. Giamarchi, *Phys. Rev. B* 78, 075124 (2008).
- <sup>21</sup> Jun-ichi Okamoto and A. J. Millis, *Phys. Rev. B* 85, 115406 (2012).
- <sup>22</sup> David Carpentier and Edmond Orignac, *Phys. Rev. B* 74, 085409 (2012).
- <sup>23</sup> Thierry Giamarchi, *Quantum physics in one dimension*, Clarendon Press (2003).
- <sup>24</sup> John Cardy, *Scaling and renormalization group in statistical physics*, Cambridge University Press (1996).
- <sup>25</sup> Alexander Altland and Ben D. Simons, *Condensed matter field theory*, Cambridge University Press (2010).
- <sup>26</sup> Xi Dai, Zhong Fang, Yi Zhou, and Fu-Chun Zhang, *Phys. Rev. Lett.* 101, 057008 (2008).
- <sup>27</sup> P. Fulde and R. A. Ferrell, *Phys. Rev.* 135, A550 (1964).
- <sup>28</sup> A. I. Larkin and Y. N. Ovchinnikov, *Zh. Eksp. Teor. Fiz.* 47, 1136 (1964), [*Sov. Phys. JETP* 20, 762 (1965)].
- <sup>29</sup> N. D. Mermin and H. Wagner, *Phys. Rev. Lett.* 17, 1133 (1966).
- <sup>30</sup> P.C. Hohenberg, *Phys. Rev.* 158, 383 (1967).